Journal of Medicinal Chemistry

pubs.acs.org/jmc Article

Single Diastereomers of the Clinical Anticancer ProTide Agents NUC-1031 and NUC-3373 Preferentially Target Cancer Stem Cells *In Vitro*

Magdalena Slusarczyk,* Michaela Serpi, Essam Ghazaly, Benson M. Kariuki, Christopher McGuigan, and Chris Pepper*

Cite This: *J. Med. Chem.* 2021, 64, 8179–8193 Read Online

ACCESS | Metrics & More | Article Recommendations | Supporting Information

ABSTRACT: A 3′-protected route toward the synthesis of the diastereomers of clinically active ProTides, NUC-1031 and NUC-3373, is described. The *in vitro* cytotoxic activities of the individual diastereomers were found to be similar to their diastereomeric mixtures. In the KG1a cell line, NUC-1031 and NUC-3373 have preferential cytotoxic effects on leukemic stem cells (LSCs). These effects were not diastereomer-specific and were not observed with the parental nucleoside analogues gemcitabine and FUDR, respectively. In addition, NUC-1031 preferentially targeted LSCs in primary AML samples and cancer stem cells in the prostate cancer cell line, LNCaP. Although the mechanism for this remains incompletely resolved, NUC-1031-treated cells showed increased levels of triphosphate in both LSC and bulk tumor fractions. As ProTides are not dependent on nucleoside transporters, it seems possible that the LSC targeting observed with ProTides may be caused, at least in part, by preferential accumulation of metabolized nucleos(t)ide analogues.

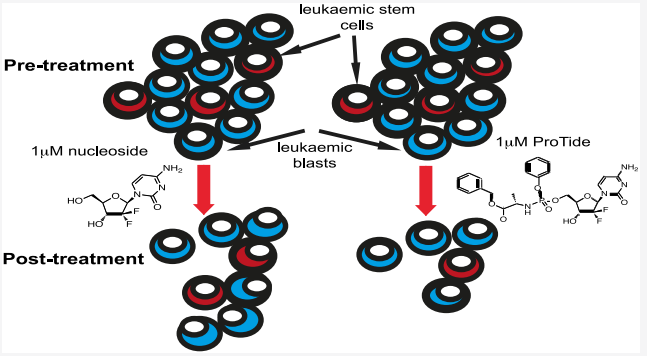

INTRODUCTION

The phosphoramidate (ProTide) approach[1] applied to antiviral and anticancer nucleoside analogues (NAs), and more recently also to non-nucleoside compounds,[2−8] continues to be of significant interest in the drug discovery field. This approach is used to overcome the limitations of NAs that are known to restrict their therapeutic potential. In the oncology arena, the application of ProTide technology to gemcitabine and floxuridine (FUDR) led to the discovery and clinical development of two anticancer agents, NUC-1031[9] and NUC-3373[10] (Figure 1). The first-in-class agent, NUC-1031, was designed to overcome the cancer cell resistance mechanisms that limit the clinical utility of gemcitabine (dFdC). The three key resistance mechanisms involve down-regulation of nucleoside transporter proteins (hENT1); down-regulation of the key initial phosphorylating enzyme deoxycytidine kinase (dCK) that is required to activate dFdC to the 5′-monophosphate form dFdCMP; and up-regulation of the catabolizing enzyme cytidine deaminase (CDA).[11−13] NUC-1031 has been assessed in four completed clinical studies, including a Phase I study in patients with advanced solid tumors (PRO-001), a Phase Ib study in patients with recurrent ovarian cancer (PRO-002), a Phase Ib study in patients with locally advanced or metastatic biliary tract cancer (BTC) (ABC-08), and a Phase II study in patients with platinum-resistant ovarian cancer (PRO-105). Two clinical studies of NUC-1031 are currently ongoing: a Phase III study in metastatic pancreatic carcinoma (ACELARATE) and a Phase III study in locally advanced or metastatic BTC (NuTide:121). Results from PRO-001 revealed that NUC-1031 has a favorable pharmacokinetic profile with a long plasma half-life (8.3 h versus 1.5 h) and can generate intracellular levels of the active anticancer metabolite dFdCTP that are 217-times higher than those generated by gemcitabine. Furthermore, NUC-1031 achieved high levels of disease control (78%) in patients who had exhausted all other treatment options, including those with tumors relapsed/refractory to prior chemotherapy with gemcitabine.[14] In June 2019, Acelarin, the NUC-1031_S_P isomer enriched API (98% S_P-isomer: 2% R_P-isomer), received orphan drug designation from the FDA for the treatment of BTC.[15] Currently, the S_P isomer of NUC-1031 is being investigated in all NUC-1031 clinical studies.

Received: December 19, 2020
Published: June 4, 2021

https://doi.org/10.1021/acs.jmedchem.0c02194
J. Med. Chem. 2021, 64, 8179–8193

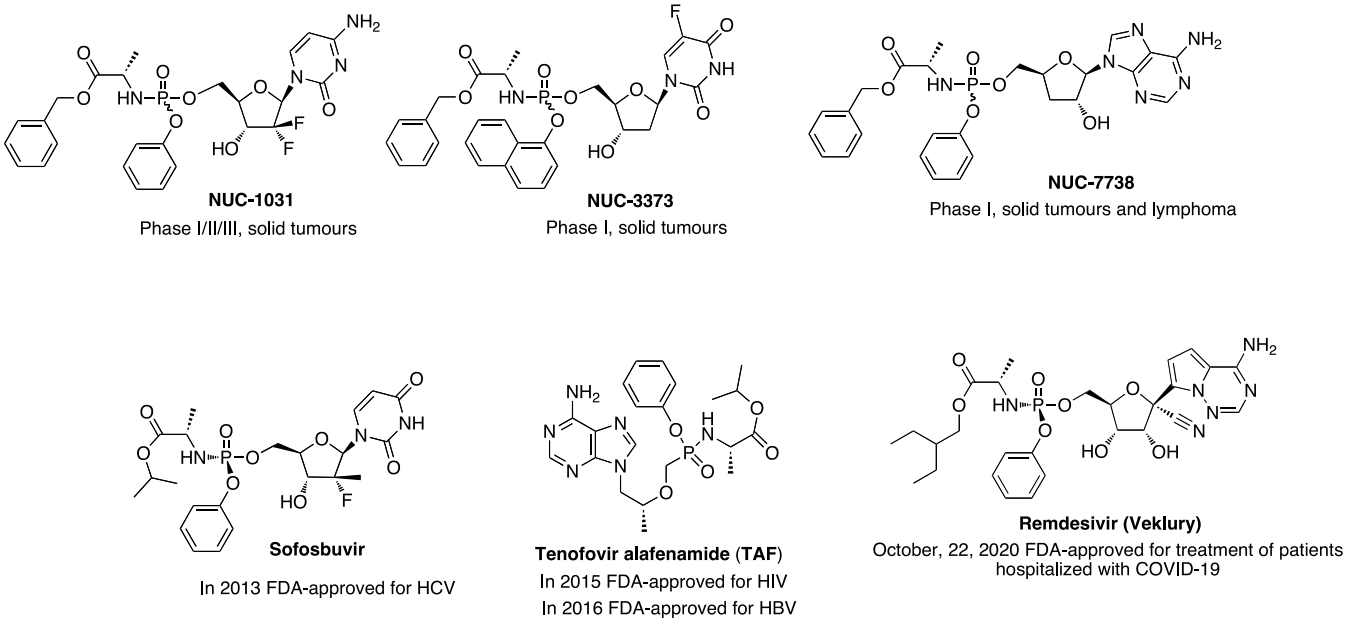

Figure 1. Phosphoramidate transformations of anticancer and FDA-approved antiviral nucleoside monophosph(on)ate analogues in the clinic and ongoing clinical studies.

The second agent, NUC-3373, is a ProTide modification of FUDR, the fluorinated pyrimidine nucleoside derivative of 5-FU. These fluoropyrimidines are established clinical drugs used in the treatment of solid tumors including gastrointestinal, kidney, ovarian, and breast cancers.[16] The key resistance mechanisms that limit 5-FU and FUDR involve down-regulation of the activating enzyme, thymidine kinase (TK), required for the first phosphorylation step that transforms FUDR to the active anticancer metabolite (FdUMP); up-regulation of thymidylate synthase (TS), which is considered to be the main target for 5-FU and FUDR; up-regulation of the degradative enzyme thymidine phosphorylase (TP); and decreased expression of nucleoside/nucleobase transport proteins.[17] In addition, more than 85% of administered 5-FU is degraded by dihydropyrimidine dehydrogenase (DPD) before it has an opportunity to enter cancer cells and exert any therapeutic effect.[18] *In vitro* data confirmed that NUC-3373 exerts its cytotoxic activity independently of thymidine kinase in TK-deficient tumor cell lines, and it is resistant to degradative action by catabolic enzymes including TP and DPD.[19] In addition, NUC-3373 was found to generate 366-fold higher intracellular levels of the active monophosphate form, FdUMP, in the human colorectal cancer cell line HT29 compared with 5-FU and achieved significantly greater tumor volume reduction than 5-FU in HT29 xenograft studies.[20] NUC-3373, as a diastereomeric mixture, is currently being assessed in two ongoing clinical studies. Interim pharmacokinetic data from the first-in-human Phase I study of NUC-3373 in patients with advanced solid tumors (NuTide:301) demonstrated that NUC-3373 has a long plasma half-life (9.7 h versus 8−14 min) and the ability to completely deplete the pool of dTMP in patients PBMCs, compared to 5-FU. A three-part Phase I study of NUC-3373 in combination with standard agents used in colorectal cancer treatment (NuTide:302) is also ongoing and is designed to identify a recommended Phase II dose (RP2D) and schedule for NUC-3373 when combined with other agents.[21] Recently, a third anticancer agent, NUC-7738, the ProTide modification of 3′-deoxyadenosine (3′-dA; also known as cordycepin), entered a Phase I clinical study.[22]

NUC-1031 and NUC-3373 ProTides were obtained via a coupling reaction between 3′-Boc-protected gemcitabine or FUDR and phosphorylating agent (phosphorochloridate) in the presence of either Grignard reagent (*tert*-butyl magnesium chloride) or *N*-methylimidazole (NMI). In both cases, the formation of a pair of diastereomers at the phosphate center (1:1 ratio S_P/R_P) was achieved and, as such, NUC-1031 and NUC-3373 were further biologically evaluated.[9,10] Although NMI favors the phosphorylation of the primary hydroxyl group at the nucleoside's 5′-position, the yield of the coupling reaction is usually low. On the contrary, the Grignard reagent is not selective, hence allowing the formation of a 5′-phosphoramidate along with undesired 3′- and 3′,5′-phosphoramidates. In order to prevent the formation of these byproducts, a selective 3′-protection of the nucleosides is required prior to the coupling reaction. This strategy involves an additional deprotection step at the 3′-positions in the obtained protected-phosphoramidates, as recently reviewed.[23] Because the yield of coupling reaction in the presence of the Grignard reagent is usually moderate to high, we adopted the hydroxyl groups protection as a strategy to prepare NUC-3373 with higher yield. In the case of gemcitabine, 3′-OH protection is more direct and selective due to the presence of fluorine atoms at the 2′-position in the sugar moiety. For FUDR, which lacks any substituents at the 2′-position, an initial protection of both 3′- and 5′-OH and subsequent selective 5′-deprotection was necessary. The 3′-OH protected FUDR was further used for a coupling reaction with a phosphorochloridate in the presence of the Grignard reagent to improve the overall yield of NUC-3373 synthesis. A variety of hydroxyl protecting groups can be used to prepare 3′-protected ProTides.[23] A *tert*-butyl silyl group (TBDMS) was selected at first and was found to be the most optimal as a clear separation of two diastereomers of the 3′-protected NUC-3373 mixture was possible by normal-phase chromatography. Although a regioselective strategy to obtain the desired 5′-ProTides was

https://doi.org/10.1021/acs.jmedchem.0c02194
J. Med. Chem. 2021, 64, 8179−8193

published,[24] during the course of the present study, we decided to proceed with our alternative methodology and to separate a mixture of two diastereomers at the level of 3′-protected ProTides. This alternative approach was of particular interest in light of the notable difference in activity between S_P and R_P isomers discovered for FDA-approved antiviral ProTide agents sofosbuvir[25] (18-fold increase in potency against HCV for the S_P isomer)[26] and TAF[27] (10-fold increase in potency against HIV for the S_P isomer)[28] (Figure 1). In fact, chirality and chiral separation of racemic compounds are considered important topics in drug development. Most isomers of chiral drugs, including diastereomers, differ in their pharmacology, pharmacokinetics, metabolism, and biological activities.[29] With this in mind, the current FDA recommendation is to assess activity of each isomer of racemic therapeutic agents.[30] Over the past decade, different diastereoselective methods for the synthesis of *P*-chirogenic phosphoramidates have been developed, including methods using a chiral auxiliary-bearing phosphoramidating reagent,[31] diastereomerically pure phosphoramidating agent with *p*-nitro-phenyl or 2,3,4,5,6-pentafluorophenyl as leaving aryloxy groups,[32,33] or a method based on the process for the diastereomeric enrichment due to differences in solubility of S_P and R_P diastereomers in alcohols.[34]

In our laboratory, we have focused on the development of diastereoselective synthetic methods via a copper-catalyzed reaction in the presence of different bases.[35] Additionally, methods for the separation of 3′-protected ProTides as a diastereomeric mixture, in general being very difficult to isolate as single diastereomers by standard chromatography (reverse-phase chromatography or crystallization), were probed.

Herein, we report an alternative synthetic procedure to obtain S_P and R_P isomers of the two clinical anticancer agents NUC-3373 and NUC-1031. A selective TBDMS-protection and deprotection manipulation of FUDR and gemcitabine was followed by a coupling reaction to give 3′-protected phosphoramidates which were separated to single diastereomers. Further removal of 3′-TBDMS group in each separated isomer yielded NUC-3373 and NUC-1031 as single isomers. NUC-1031 diastereomers were obtained upon column chromatography in crystalline form and the stereochemistry at the phosphorus center was assigned via X-ray crystallography. Moreover, for the first time, we disclose *in vitro* biological data for single R_P and S_P isomers of NUC-1031 and NUC-3373 (stereochemistry to be determined) as well as their ability to target cancer stem cells (CSC).

RESULTS AND DISCUSSION

Chemistry. The selective protection and deprotection of hydroxyl groups in nucleoside analogues subjected to ProTide technology and the coupling reaction represents a solid strategy to improve the overall yield of phosphoramidate synthesis. This alternative approach may be considered as advantageous over the general method in which nonprotected nucleoside starting materials are used, as only the desired 5′-phosphorylated ProTides are formed. The alternative procedure for the preparation of clinical anticancer agents NUC-3373 and NUC-1031 from 3′-protected FUDR and gemcitabine, respectively, is depicted in general in Scheme 1. In our approach to improve the efficiency of the route to obtain the desired 5′-ProTides, we selected the *tert*-butyldimethyl silyl group reported for its ability to be selectively cleaved from the primary TBDMS hydroxyl groups

Scheme 1. General Synthetic Strategy Toward 3′-TBDMS-Protected Nucleosides 5 and 6[a]

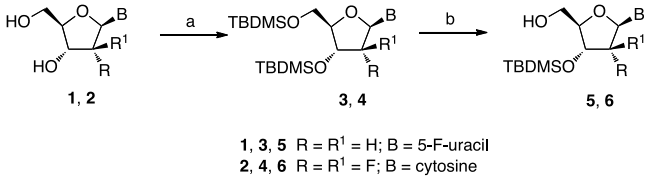

[a]Reagents and conditions: (a) imidazole (5.0 equiv), TBDMSCl (2.2 equiv), DMAP (0.3 equiv), DMF, 0 °C to rt, 1 h; (b) CSA (1.0 equiv), MeOH, rt, 10 min or TCA (28.0 equiv), THF, H_2O, rt, 2 h.

in the presence of their secondary equivalents.[36] Thus, first FUDR (**1**) was treated with TBDMS, imidazole, and DMAP at elevated temperature[37] to give the 5′,3′-TBDMS protected FUDR derivative (**3**) in 98% yield. Next, the FUDR intermediate **3** was subjected to different deprotection conditions to selectively remove the 5′-TBDMS moiety. The primary silyloxy groups are known to be cleaved under acidic conditions more efficiently in comparison with their secondary counterparts. Therefore, we investigated a variety of acidic conditions starting with a TFA/H_2O/THF (1:1:4) mixture, reported by Zhu et al. as the most suitable for selective 5′-desilylation of the multisilylated nucleoside analogues.[36] However, when compound **3** was treated under the above-mentioned conditions, 3′-TBDMS-FUDR derivative (**5**) was obtained in low yield (20%). Due to poor selectivity of trifluoroacetic acid toward 5′-desilylation, different acids such as *p*-toluenesulfonic acid (*p*-TsOH) or camphorsulfonic acid (CSA) were further tested as summarized in Table 1. No selectivity was observed when desilylation was performed with 0.6 equiv of *p*-TsOH in methanol at room temperature. After 1 h of reaction, a mixture of 3′- and 5′-monosilylated products in almost 1:1 ratio were detected along with a significant amount of starting material **3** (entry 1, Table 1). Decreasing the reaction temperature to −15 °C considerably improved the selectivity, and the desired product **5** was recovered in 45% yield after 4 h (entry 2, Table 1). Replacing MeOH with DCM drastically slowed down the reaction and significantly decreased the 5′-desilylation selectivity (data not reported). The yields were estimated by ^{1}H and ^{19}F NMR of the crude reaction mixture. Given the unsatisfactory result obtained with *p*-TsOH, we turned our attention to a new strategy with 10-camphorsulfonic acid (CSA), which has been reported in a few cases to be able to selectively deprotect primary silyl ether in multisilylated nucleosides to give free primary alcohol.[37,38] Thus, when the reaction was carried out in a 1:1 mixture of DCM/MeOH at low temperature (0−5 °C), slow deprotection was detected; however, a remarkable selectivity was observed. The desired compound **5** was obtained in 38% crude yield as estimated by ^{1}H and ^{19}F NMR. By increasing the temperature to 25 °C, the selectivity toward 5′-desilylation was retained and the reaction was completed within 2.5 h, providing compound **5** with 37% yield (data not shown). A major improvement was obtained when only MeOH was employed as a solvent. In this case the reaction was accomplished much faster, and after 1 h the desired compound **5** was formed in 60% crude yield based on ^{1}H and ^{19}F NMR (entry 5, Table 1). Performing the reaction under the same conditions but at room temperature increased the rate of the deprotection. However, after 45 min, a significant amount of FUDR was formed, suggesting that meticulous monitoring is

https://doi.org/10.1021/acs.jmedchem.0c02194
J. Med. Chem. 2021, 64, 8179−8193

Table 1. Selective 5′-Desilylation of 3′,5′-TBDMS-FUDR (3) and 3′,5′-TBDMS-Gemcitabine (4): Conditions Optimization

entry	nucleoside analogue	acid/equiv	solvent	time/temp	yield[a,b] (%)
1	FUDR	*p*-TsOH/0.6	MeOH	1 h/rt	
2	FUDR	*p*-TsOH/1.0	MeOH	4 h/−15 °C	45[a]
3	FUDR	*p*-TsOH/1.0	DCM	6 h/15 °C−rt	
4	FUDR	CSA/0.6	MeOH	30 min/0 °C	56[a]
5	FUDR	CSA/0.6	MeOH	1 h/0 °C	60[a]
6	FUDR	CSA/0.5	MeOH	25 min/rt	50[b]
7	FUDR	CSA/0.6	MeOH	45 min/rt	
8	FUDR	CSA/1.0	MeOH	10 min/rt	60[b]
9	FUDR	CSA/1.0	AcCN	1 h/rt	
10	FUDR	CSA/1.0	acetone	10 min/rt	
11	gemcitabine	CSA/1.0	MeOH	10 min/rt	
12	gemcitabine	TCA/28.0	THF/H_2O	30 min/rt	82[b]

[a]5′-Desilylated product, calculated yield by ^{1}H and ^{19}F NMR. [b]Isolated yield.

required (entry 7, Table 1). The best result was obtained when performing the reaction in MeOH with 1 equiv of CSA at room temperature in 10 min. Under these conditions the desired product **5** was recovered after work up in 60% yield (entry 8, Table 1). Additional attempts to improve the yield of 5′-TBDMS removal by changing solvents were unsuccessful (entries 9 and 10, Table 1).

Next, the same conditions for protection and selective 5′-deprotection were applied to gemcitabine (**2**) to form the key intermediate **6**. However, instead of 3′-TBDMS-protected gemcitabine **6**, formation of its 5′-TBDMS-protected analogue was observed along with the starting bis-silylated compound **4**. While an attempt to selectively remove a silyl group from the 5′-position with oxalic acid (up to 3.0 equiv) was found unsuccessful (data not reported), the use of trichloroacetic acid (28 equiv) in a mixture of THF/H_2O (3.5:1) gave the key intermediate **6** with 82% yield (entry 12, Table 1).

The key intermediate **5** was further subjected to the standard coupling conditions with L-Ala-OBn-ONaph phosphorochloridate[10] in the presence of the Grignard reagent (Scheme 2). 3′-TBDMS-protected compound 7 obtained as a mixture of diastereomers was purified using normal-phase chromatography to give single isomers: fast eluting (**7_isomer A**, **7a** or **7b**) and slow eluting (**7_isomer B**, **7a** or **7b**). A final deprotection of the 3′-silyl group in isomers **7a** and **7b** was performed with a 4:1:1 mixture of THF/TFA/H_2O at 0 °C and yielded single diastereomers of NUC-3373, herein reported as NUC-3373_isoA (**9a** or **9b**) (obtained from **7_isoA**) and NUC-3373_isoB (**9a** or **9b**) (obtained from **7_isoB**) as stereochemistry at the phosphorus atom remained undetermined at the time of preparation of this manuscript. Attempts to crystallize NUC-3373_isoA (**9a** or **9b**) and NUC-3373_isoB (**9a** or **9b**) as well as their 3′-protected precursors (**7_isomer A** and **7_isomer B**) from various solvents including MeOH, 2-propanol, $CHCl_3$ and a combination of $CHCl_3$/Et_2O (1:1), and MeOH/$CHCl_3$ (3:1), $CHCl_3$/H_2O (1:1) were unsuccessful. In addition, the vapor diffusion method, using 2-propanol/hexane, MeOH/H_2O and MeOH/petroleum ether as the binary solvent system, did not lead to formation of crystalline form. In parallel, a coupling reaction between L-Ala-OBn-OPh phosphorochloridate[9] and **6** gave 3′-TBDMS-protected NUC-1031 analogue **8**, further isolated as single isomers **8a** and **8b** via column chromatography. Removal of the 3′-TBDMS-group in separated diastereomers **8a** and **8b** under acidic conditions provided isomers of NUC-1031 **10a** and **10b** (Scheme 2), which after normal-phase chromatography were obtained as a crystalline solid. The molecular structure and stereochemistry at the phosphate center was elucidated by single-crystal X-ray crystallography for the two isomers of NUC-1031 and determined to be S_P and R_P for diastereomers **10a** and **10b**, respectively (Figure 2).

Scheme 2. General Synthetic Strategy Toward Separated Diastereomers of NUC-3373 and NUC-1031 (9a,9b and 10a,10b)[a]

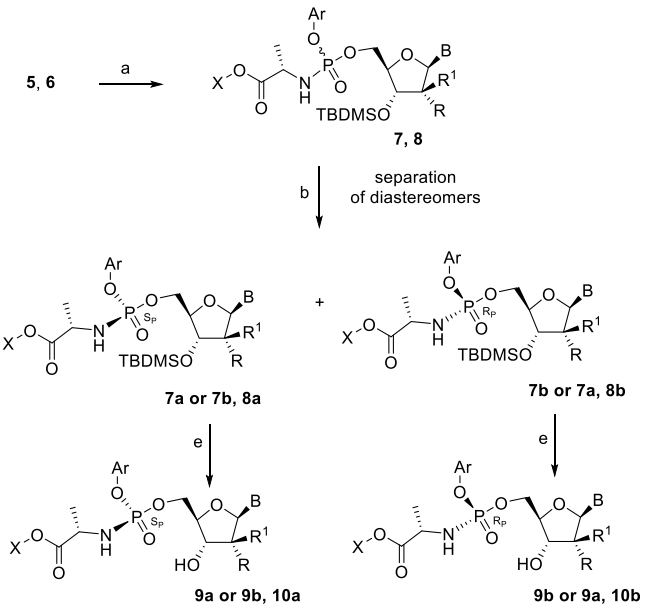

[a]Reagents and conditions: (a) (ArO)(XOC(O)CHCH$_3$NH)P(O)Cl (2.0 equiv), *tert*-BuMgCl, THF, rt, 16 h; (b) separation of diastereomers; and (c) THF/TFA/DCM (4:1:1), 0 °C for 2 h, then rt for 12 h.

***In Vitro* Cytotoxic Activity.** The single isomers of NUC-1031 and NUC-3373 were biologically evaluated for cytotoxic activity in a panel of solid tumor cell lines (Mia-Pa-Ca-2, Bx-PC-3, LNCaP, HT-29, HCT-116, MDA-MB-231, and SW-620), the acute myeloid leukemia (AML) cell line, KG1a, and primary AML blasts. The activity of the ProTides was compared with the corresponding diastereomeric mixtures NUC-3373 and NUC-1031 as well as with the parent nucleosides FUDR (**1**) and gemcitabine (**2**), respectively

https://doi.org/10.1021/acs.jmedchem.0c02194
J. Med. Chem. 2021, 64, 8179−8193

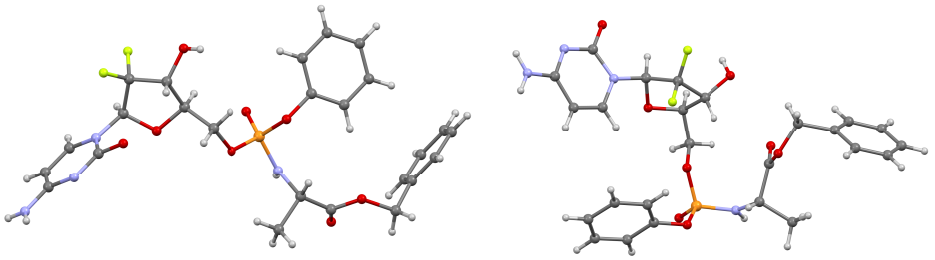

Figure 2. X-ray crystal structures of **10a** (NUC-1031_S_P) and **10b** (NUC-1031_R_P).

Table 2. Cytotoxicity of NUC-3373 and NUC-1031 as a Diastereomeric Mixture and Single Isomers R_P and S_P Reported as LC_{50} (μM) Values[a]

	LC_{50}(μM) ± SEM in different cell lines							
cmpd	Mia-Pa-Ca-2[a]	Bx-PC-3[a]	LNCaP	HT-29	HCT-116	SW-620[a]	MDA-MB-231	KG1a
5-FU				5.5 ± 0.8	3.7 ± 0.7	7.98	12.6 ± 1.1	1.4 ± 0.5
FUDR				0.8 ± 0.3	1.6 ± 0.4	1.55	2.4 ± 0.7	1.18 ± 0.4
NUC-3373				1.7 ± 0.6	3.1 ± 0.8	1.84	2.8 ± 0.9	0.053 ± 0.02
NUC-3373_IsoA (**9a** or **9b**)				2.1 ± 0.6	4.3 ± 1.0	2.37	3.6 ± 0.6	0.052 ± 0.01
NUC-3373_IsoB (**9a** or **9b**)				1.5 ± 0.4	2.6 ± 0.9	1.46	2.5 ± 0.6	0.055 ± 0.02
gemcitabine	0.01	0.74	2.8 ± 0.5	0.7 ± 0.2				1.8 ± 0.3
NUC-1031	0.1	2.29	3.1 ± 0.6	1.3 ± 0.5				0.28 ± 0.07
NUC-1031_S_P(**10a**)	0.03	2.44	2.6 ± 0.7	1.5 ± 0.3				0.31 ± 0.1
NUC-1031_R_P(**10b**)	0.19	1.29	3.4 ± 0.5	1.0 ± 0.4				0.25 ± 0.1

[a]LC_{50} values (the concentration of drug required to induce 50% cell death) were calculated using an MTS assay performed in duplicate and tested in 9 serial concentrations from 198 μM to 0.0199 μM (data expressed as mean LC_{50} values) or an Annexin V/7-AAD assay performed in triplicate (data expressed as mean LC_{50} values ± SEM).

(Table 2). In the solid tumor cell lines, the LC_{50} values for both NUC-3373 isomers were comparable to those of NUC-3373 and FUDR and ranged between 0.61−2.37 μM and 0.31−1.46 μM in HT-29 and SW-620 for NUC-3373_IsoA (**9a** or **9b**) and NUC-3373_IsoB (**9a** or **9b**), respectively. In comparison to 5-FU, a significant increase in potency was observed and ranged between 13 and 25-fold and 3−5-fold for NUC-3373_IsoA (**9a** or **9b**) and NUC-3373_IsoB (**9a** or **9b**), respectively, in HT-29 and SW-620 cell lines. The cytotoxic activity of the gemcitabine ProTide NUC-1031 and its isomers were similar, except for the NUC-1031_S_P isomer (**10a**) in the Mia-Pa-Ca-2 cell line, which was found to be 6-fold more potent than its R_P analogue **10b** (0.03 μM vs 0.19 μM) and 3-fold more potent than its diastereomeric mixture (0.03 μM vs 0.10 μM). In the HT-29 cancer cell line, the submicromolar LC_{50} values for both S_P and R_P NUC-1031 isomers and NUC-1031 ranged between 0.34 and 0.74 μM, similar to the gemcitabine LC_{50} value of 0.21 μM. NUC-1031 and both isomers were equipotent in the Bx-PC-3 tumor cell line. When considering the KG1a cell line, NUC-1031 was approximately 6-fold more potent than gemcitabine, again, with no significant difference between the diastereomers (Figure 3A−C). We went on to confirm that NUC-1031 was significantly more potent than gemcitabine in primary AML blasts (Figure 3G,H). Similarly, NUC-3373 was approximately 23-fold more potent than FUDR with no significant difference between the diastereomers (Figure 3D−F).

The metabolic stability of NUC-3373, NUC-1031, and the separated diastereomers (**9a**, **9b** and **10a**,**10b**) was investigated by incubation with human hepatocytes. The half-lives and percentage of compounds remaining after 1 h were measured and are outlined in Table 3. In human hepatocytes, NUC-3373_IsoA (**9a** or **9b**) was found to be slightly more stable than NUC-3373_IsoB (**9a** or **9b**) and its diastereomeric mixture NUC-3373, with a half-life of 53 min. In the case of the gemcitabine family, NUC-1031_S_P (**10a**) was found to have a shorter half-life of 37 min in human hepatocytes compared with NUC-1031_R_P (**10b**), which had a half-life >120 min. This intriguing discrepancy in half-life of both NUC-1031 isomers in human hepatocytes could potentially be explained by different carboxylesterases (CESs) substrate specificity also toward isomers. Mammalian carboxylesterases (CES1 and CES2), the crucial enzymes involved in the metabolism of endogenous esters and ester or amide-containing xenobiotics, may exhibit different hydrolysis rate between the *R*- and *S*-isomers. Thus, their reactivity might be affected by the conformational orientation into the active pocket of CESs.[39]

Biological Activation: Carboxypeptidase Y Assay. The mechanism of activation of NUC-1031 and NUC-3373 in their diastereomeric forms was previously reported[9,10] and was confirmed to follow the commonly accepted putative route (Scheme 3). The activation pathway involves (i) carboxypeptidase-mediated hydrolysis of the ProTide ester moiety to form the intermediate **A**, (ii) displacement of the aryl moiety and spontaneous cyclization of **A** to form metabolite **B**, and (iii) spontaneous hydrolysis of cyclic anhydride **B** to the intermediate **C**. The latter metabolite would then be converted to the monophosphate **D** via P−N bond cleavage catalyzed by a phosphoramidase-type enzyme. In this work, we carried out an enzymatic assay for the two separated isomers NUC-3373_isoA (**9a** or **9b**) and NUC-3373_isoB (**9a** or **9b**) and for the gemcitabine ProTide NUC-1031_S_P (**10a**) and NUC-1031_R_P (**10b**) in the presence of carboxypeptidase Y

https://doi.org/10.1021/acs.jmedchem.0c02194
J. Med. Chem. 2021, 64, 8179−8193

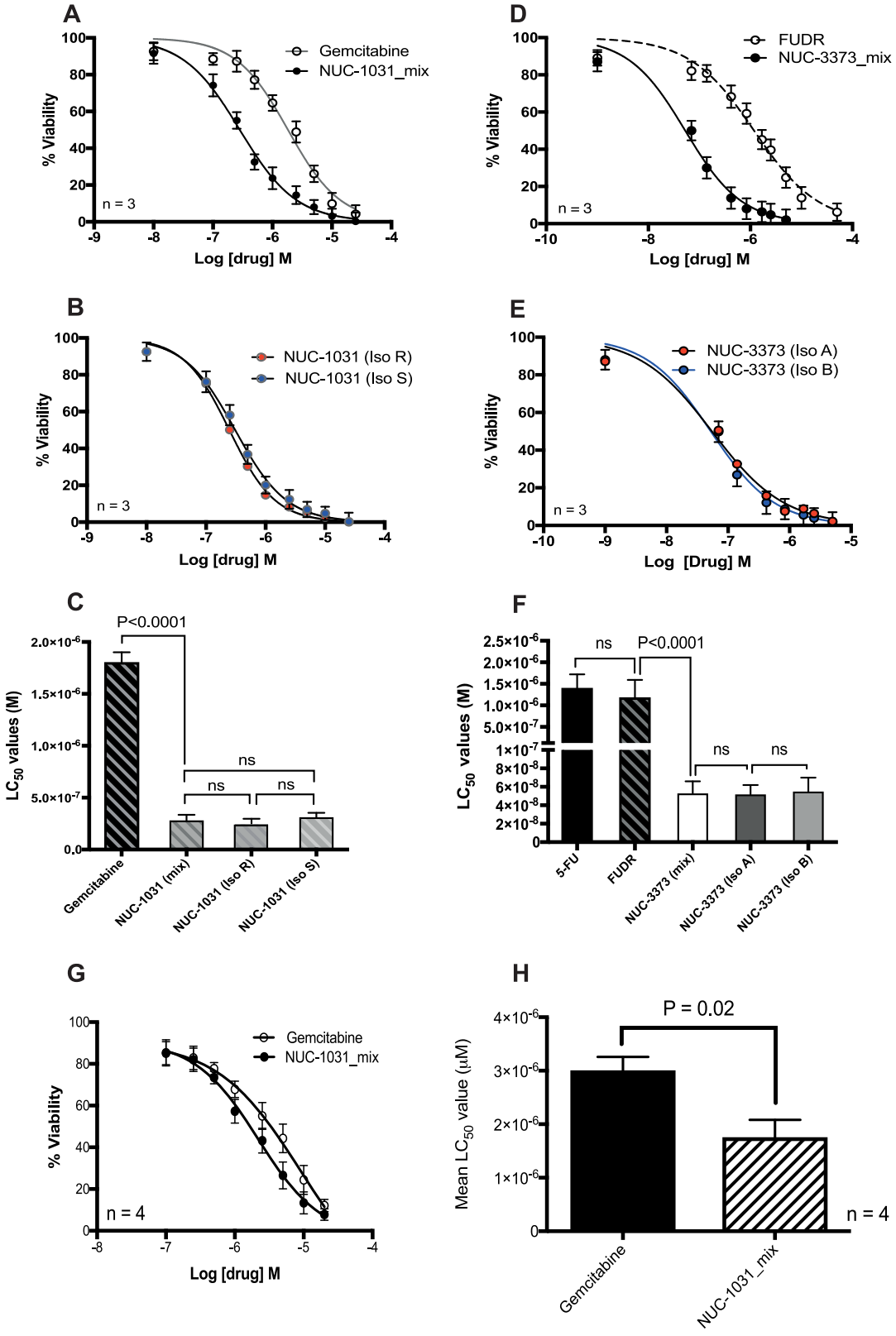

Figure 3. Overlaid sigmoidal dose−response curves. (A) Comparison of gemcitabine and NUC-1031_mix (diasteromeric mixture) and (B) the separated diastereomers, NUC-1031_S_P (**10a**) and NUC-1031_R_P (**10b**). (C) Comparison of the LD_{50} values for gemcitabine, NUC-1031_mix, NUC-1031_S_P (**10a**), NUC-1031_R_P (**10b**). (D) Comparison of FUDR and NUC-3373_mix (diasteromeric mixture) and (E) the separated diastereomers NUC-3373_isoA (**9a** or **9b**) and NUC-3373_isoB (**9a** or **9b**). (F) Comparison of the LD_{50} values for 5-FU, FUDR, NUC-3373_mix, NUC-3373_isoA (**9a** or **9b**), and NUC-3373_isoB (**9a** or **9b**). All assays carried out using KG1a cells are presented as mean (±SEM) of five independent experiments. (G,H) Relative sensitivity of primary AML blasts to gemcitabine and NUC-1031_mix (n = 4).

https://doi.org/10.1021/acs.jmedchem.0c02194
J. Med. Chem. 2021, 64, 8179−8193

Table 3. Metabolic Stability of ProTides Incubated with Human Hepatocytes

intrinsic clearance (cryopreserved human hepatocytes)		
cmpd	half-life (min)	% compound remaining after 1 h
NUC-3373	34	30
NUC-3373_IsoA (**9a** or **9b**)	53	40
NUC-3373_IsoB (**9a** or **9b**)	47	40
NUC-1031	76	58
NUC-1031_S_P (**10a**)	37	33
NUC-1031_R_P (**10b**)	>120	97

according to the standard procedure.[40] Within 10 min of incubation (Figure 4), NUC-3373_isoA (**9a** or **9b**) was fully processed to metabolite **A**, as indicated by the lack of the single peak at δ 4.04 ppm ascribed to the NUC-3373_isoA (**9a** or **9b**) and appearance of a single peak at δ 5.16 ppm (metabolite **A**). During this time, a single peak at δ 6.80 ppm corresponding to achiral metabolite **C** was also detected. Slightly slower processing to metabolites **A** and **C** was observed for the isomer NUC-3373_isoB (**9a** or **9b**) within the first 10 min of incubation, during which 28% of NUC-3383_isoB remained unprocessed by the enzyme (Supporting Information, Figure S1a).

In the case of the gemcitabine ProTide NUC-1031, only the S_P isomer (**10a**) was processed to its metabolites **A** (δ 4.51 ppm, 68%) and **C** (δ 6.80 ppm, 18%) within the first 10 min of incubation with carboxypeptidase Y. NUC-1031_R_P (**10b**) was converted to metabolite **C** (without metabolite **A** detection) within approximately 120 min (Supporting Information, Figure S1b,c).

CANCER STEM CELL TARGETING

The putative existence of cancer stem cells (CSCs) has been suggested in many human cancers, including leukemias and solid tumors. The cancer stem cell hypothesis postulates that only a small subpopulation of tumor cells are responsible for tumor formation, maintenance of the bulk of the tumor, as well as its invasion and metastasis. In 1994, Lapidot and co-workers demonstrated that only a small percentage of acute myeloid leukemia cells had the capability to initiate leukemia in mice.[41] These leukemic stem cells (LSCs) were shown to express similar cell surface markers ($CD34^+/CD38^-$) to normal hematopoietic stem cells implying that a similar hierarchical organization may occur in tumors. Subsequently, CSCs have been found in a wide range of solid tumors including breast, lung, colon, prostate, ovarian, skin, and pancreas.[42] CSCs are also linked with the development of resistance to therapy and recurrence of cancer, as reported for human colon cancer cell resistance to 5-FU *in vitro*[43] and for human pancreatic adenocarcinoma resistance to gemcitabine.[44]

Preferential Targeting of Cancer Stem Cells by ProTides. Given the growing interest in the treatment of cancer by targeting tumor stem cells, we assessed the relative abilities of NUC-1031_mix and NUC-3373_mix, their single diastereomers, and the parental nucleoside analogues to preferentially kill LSCs (as defined by the phenotype $CD34^+CD38^-$) in the acute myeloid leukemia cell line, KG1a, and in primary AML blasts.[45] Figure 5A,B shows that gemcitabine did not significantly alter the percentage of LSCs in the KG1a cell cultures at concentrations $\leq 2.5 \times 10^{-6}$ M. In contrast, the NUC-1031 diastereomers significantly reduced the LSC fraction at concentrations $\geq 2.5 \times 10^{-7}$ M; both diastereomers had a similar effect (Figure 5B). Importantly, we were also able to demonstrate that NUC-1031_mix preferentially depleted LSCs in primary AML blasts (Figure 5C). Furthermore, consistent with the results generated with gemcitabine, neither 5-FU nor FUDR showed any preferential toxic effect on LSCs when compared to the bulk tumor at concentrations $\leq 5 \times 10^{-6}$ M (Figure 5D). In contrast, both NUC-3373 diastereomers preferentially depleted the LSC compartment at concentrations $\geq 7 \times 10^{-8}$ M (Figure 5D). In order to establish whether this phenomenon was specific for KG1a cells and AML blasts, the prostate cancer cell line, LNCaP, was employed as an alternative cancer stem cell model. In this case, the cancer stem cells were identified by a $CD44^+CD133^+$ phenotype; this population of cells accounted for just 1.4% of the cell line. Although the LC_{50} values for gemcitabine and NUC-1031 were not significantly different ($P = 0.24$), NUC-1031 showed a preferential effect on cancer stem cell population when compared to gemcitabine at concentrations $\geq 2.5 \times 10^{-6}$ M (Figure 5E).

Intracellular Triphosphate Accumulation and ABC Transporter Expression. LSC and bulk tumor fractions (5×10^6) were isolated by high-speed cell sorting and were

Scheme 3. General Metabolic Activation Pathway for NUC-3373 and NUC-1031 ProTides

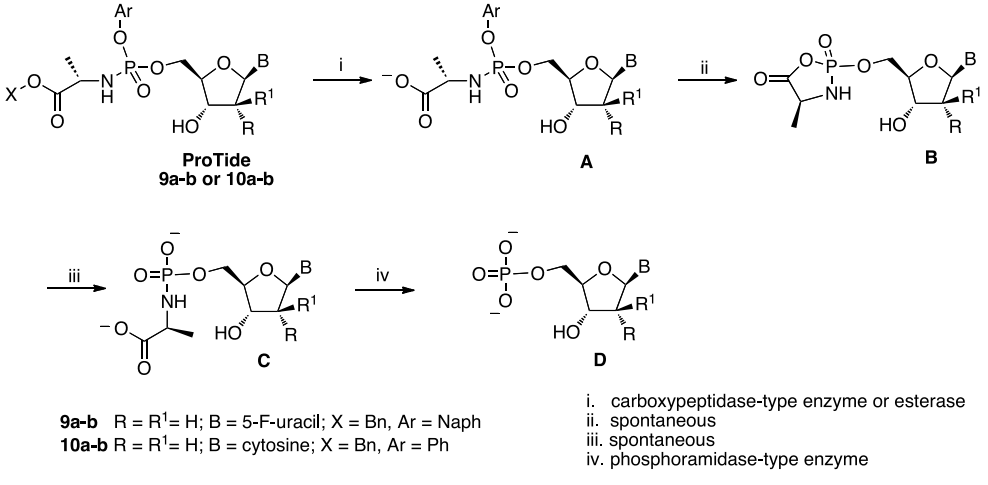

https://doi.org/10.1021/acs.jmedchem.0c02194
J. Med. Chem. 2021, 64, 8179−8193

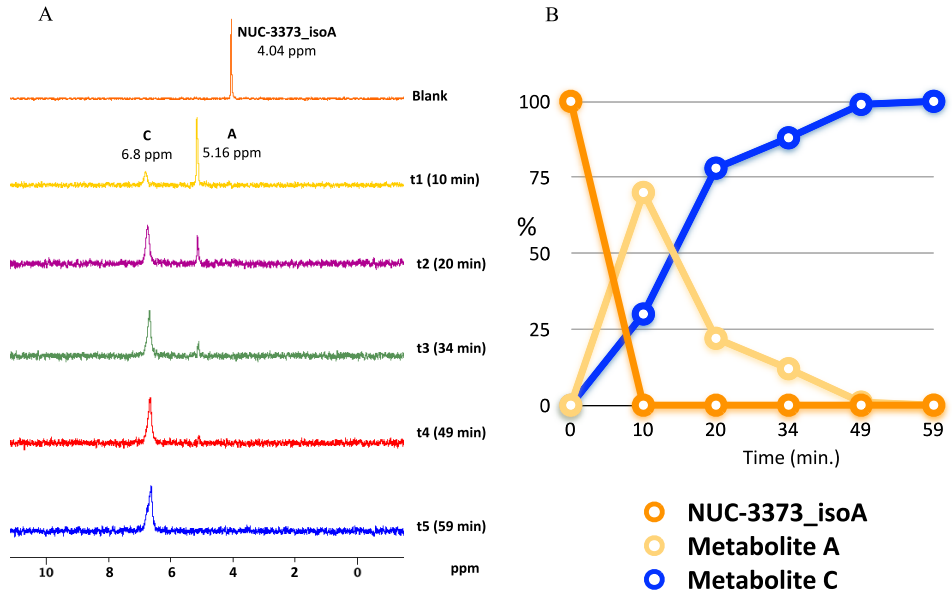

Figure 4. (A) ^{31}P NMR spectra of NUC-3373_isoA (**9a** or **9b**) over time after enzymatic incubation with carboxypeptidase Y. (B) Chart representation of percentage of NUC-3373_isoA (**9a** or **9b**) and metabolites **A** and **C** over time after enzymatic incubation with carboxypeptidase Y. Conditions 202 MHz, 25 °C, d_6-acetone, 0.05 M Trizma buffer, pH 7.6.

subsequently cultured for 1 h with either 1 μM gemcitabine or 1 μM NUC-1031_mix. The level of intracellular triphosphate was assessed using mass spectrometry and quantified by running defined concentrations of nucleoside through the mass spectrometer in order to construct a standard curve (Figure 6A). In both fractions, NUC-1031 resulted in higher intracellular accumulation of the triphosphate when compared to the parental gemcitabine nucleoside (Figure 6B). Furthermore, the LSC fraction retained high levels of the triphosphate following treatment with NUC-1031_mix, which may contribute to the preferential depletion of these cells when exposed to ProTide. In contrast, LSCs treated with gemcitabine showed approximately a 30% reduction in intracellular triphosphate when compared with bulk tumor cells. Based on the intracellular triphosphate data, we next evaluated the expression of ABC transporters in LSC and bulk tumor fractions both at the level of protein and mRNA transcript. Figure 6C shows that LSCs show a trend toward higher expression of ABCB1 and significantly higher expression of ABCG2 in LSCs versus bulk tumor cells. Furthermore, at the level of transcript, ABCB1, ABCG2, ABCC4, and ABCC5 all showed significantly increased expression in LSCs versus bulk tumor cells (Figure 6D). A number of these transporters have been previously implicated in gemcitabine resistance.[46,47]

CONCLUSION

The biological potencies and activities of single enantiomers or diastereomers of chiral compounds such as phosphoramidates (ProTides), with their stereocenter at the phosphorus atom, may differ markedly. In light of the FDA recommendation to assess activity of each isomer of racemic or diastereomeric mixtures, it became even more important to develop either stereoselective synthetic strategies or separation methods to obtain the desired isomers. Herein, we described an alternative synthesis of the two clinical anticancer agents NUC-1031 and NUC-3373 via a 3′,5′-hydroxyl group protection and 5′-deprotection strategy, which allowed separation of the single S_P and R_P diastereomers. Two diastereomers of NUC-1031 were obtained in crystalline form and their molecular structure and stereochemistry at the phosphate center was assigned via X-ray crystallography. The cytotoxic activities of R_P and S_P isomers of NUC-1031 were similar and there was no significant difference in the *in vitro* potency when compared to NUC-1031 as a diastereomeric mixture. Similarly, the *in vitro* potency of NUC-3373 and its single isomers NUC-3373_isoA and NUC-3373_isoB was comparable in the cancer cell lines tested. Attempts to crystallize two diastereomers of NUC-3373 were unsuccessful at the time of preparation of this manuscript. Both NUC-1031_mix and NUC-3373_mix and their separated diastereomers were shown to preferentially target leukemic cancer stem cells, whereas the parent nucleosides gemcitabine and FUDR did not. Mechanistically, increased intracellular accumulation of triphosphate may contribute to the preferential killing of CSCs by the ProTide in contrast to the parental analogue, but other factors may also be involved. Given that one of the gemcitabine resistance mechanisms has been associated with ABC transporter expression,[46,47] we investigated their expression in LSC and bulk tumor cells. LSCs showed significantly increased expression of ABCB1, ABCG2, ABCC4, and ABCC5 at the level of transcript and increased expression of ABCG2 at the level of protein. We postulate that the increased intracellular triphosphate in ProTide-treated cells is caused, at least in part, by the differential bioavailability of the ProTide versus the parental nucleoside analogue. As LSCs preferentially express ABC transporters, the increased intracellular accumulation of triphosphate in these cells, following treatment with ProTide, results in increased cell death of these LSCs. Importantly, the same effect was observed in cancer stem cells from a prostate cancer cell line (LNCaP). As such, ProTides may prove to be an important addition to the therapeutic repertoire, particularly in the context of eradication of cancer stem cells.

EXPERIMENTAL SECTION

Materials and Methods. *Cell Lines.* KG1a, HT-29, HCT-116, LNCaP, and MDA-MB-231 cell lines were all purchased from DSMZ

https://doi.org/10.1021/acs.jmedchem.0c02194
J. Med. Chem. 2021, 64, 8179−8193

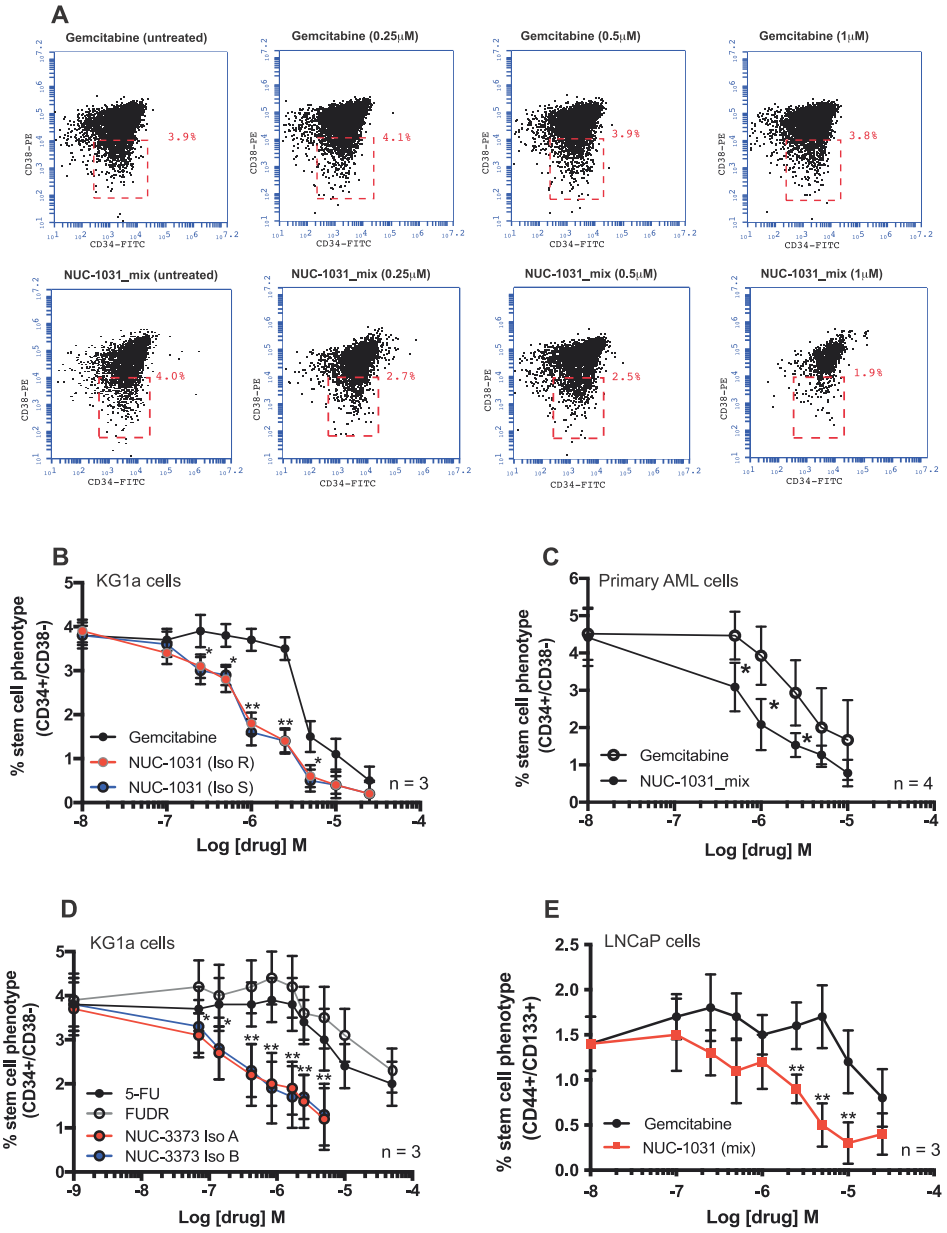

Figure 5. Differential cytotoxic effects of nucleosides and ProTides on cancer stem cells. (A) Comparison of the viable fraction of KG1a cells exposed to gemcitabine and NUC-1031_mix for 48 h. (B) Both diastereomers of NUC-1031 caused a dose-dependent, statistically significant, reduction in the LSC ($CD34^+/CD38^-$) fraction of KG1a cells. In contrast, gemcitabine had no significant effect on the LSC compartment at concentrations $\leq 2.5 \times 10^{-6}$ M. (C) The diastereomeric mixture of NUC-1031 induced a dose-dependent decrease in the LSC fraction of primary AML blasts. (D) Both diastereomers of NUC-3373 caused a dose-dependent, statistically significant reduction in the LSC ($CD34^+/CD38^-$) fraction of KG1a cells. In contrast, 5-FU and FUDR had no significant effect on the LSC compartment at concentrations $\leq 5 \times 10^{-6}$ M. $^*P < 0.05$, $^{**}P < 0.01$. (E) A similar effect was observed in the prostate cancer cell line, LNCaP. NUC-1031 preferentially depleted the cancer stem cells ($CD44^+/CD133^+$) at concentrations $\geq 2.5 \times 10^{-6}$ M when compared with gemcitabine.

(Germany). All lines were initially expanded and then frozen down in aliquots (10^7 cells) at low passage number. Cell lines were never expanded beyond 8−10 passages and were routinely confirmed as mycoplasma-free to ensure the integrity of each cell line.

MTS Cell Viability Assay. The assay was contracted and carried-out by WuXi AppTec (Shanghai) Co., Ltd. The tumor cell lines Mia-PaCa-2, Bx-PC-3, HT-29, and SW620 were seeded at cell densities of 0.5 to 100 × 10^3 cells/well in a 96-well plate the day before drug incubation. Then the plates were incubated for 72 h with the different concentrations of compound to be tested. After the incubation period, 50 μL of MTS was added and the tumor cells were incubated for 4 h at 37 °C. The data were read and collected by a Spectra Max 340 absorbance microplate reader. The compounds were tested in duplicate with 9 serial concentrations (3.16-fold titrations with 198 μM as the highest concentration), and the data were analyzed by XL-fit software.

Annexin V/7-AAD Cell Viability Assay. Cell lines were grown in T175 flasks until confluent. Cells were then aliquoted (10^5 cells/100 μL) into 96-well plates and were incubated at 37 °C in a humidified 5% CO_2 atmosphere for 72 h in the presence of tested compounds at the concentrations that were experimentally determined for each compound. In addition, control cultures were set up to which no drug was added. Cells were subsequently harvested by centrifugation and were analyzed by flow cytometry using the Annexin V/7-AAD assay. All experiments were performed in triplicate. LC_{50} values (the concentration of compound required to kill 50% of the cells in

https://doi.org/10.1021/acs.jmedchem.0c02194
J. Med. Chem. 2021, 64, 8179−8193

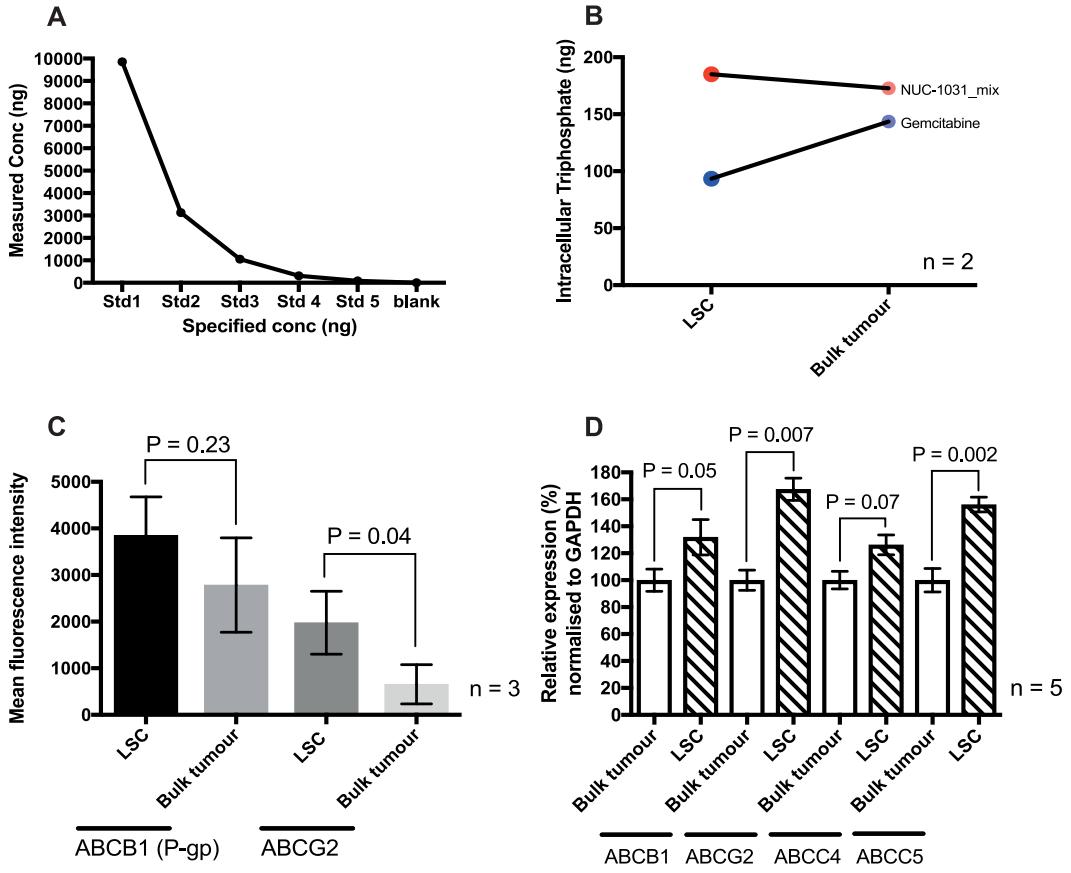

Figure 6. Measurement of intracellular triphosphate ABC transporters in LSC and bulk tumor cell fractions from KG1a cells. (A) Defined concentrations of nucleoside were run through the mass spectrometer in order to construct a standard curve (B) Purified LSCs and bulk tumor cells were treated with 1 μM of gemcitabine or NUC-1031_mix for 1 h prior to cell lysis and mass spectrometry. Both LSC and bulk tumor fractions showed increased intracellular triphosphate following treatment with NUC-1031_mix. (C) Protein expression of ABCB1 and ABCG2 on purified bulk tumor ($CD34^+/CD38^+$) and LSCs ($CD34^+/CD38^-$). Cell sorted LSCs showed significantly higher levels of ABCG2 when compared with bulk tumor cells. (D) Relative gene transcription of ABC transporter genes in purified bulk tumor cells (solid bars) and LSCs (hatched bars). LSCs showed significantly increased relative transcription of ABCB1, ABCG2, and ABCC5 when compared with bulk tumor cells. All data are the mean (±SEM) of five independent experiments, performed in triplicate.

culture) were calculated by nonlinear regression modeling using GraphPad Prism software and are shown as mean ± SEM for each replicate data set.

Metabolic Stability (Cryopreserved Hepatocytes, Human) Assay. The assay was contracted and performed by Cerep (Seattle, WA, USA Laboratories, 15318 N. E. 95th Street Redmond, WA, 98052, U.S.) according to the published procedure (Cerep ref. 1432). Pooled cryopreserved hepatocytes were thawed, washed, and resuspended in Krebs−Heinslet buffer (pH 7.3). The reaction was initiated by adding the test compound (1 μM final concentration) into cell suspension and incubated in a final volume of 100 μL on a flat-bottom 96-well plate for 0 and 60 min, respectively, at 37 °C/5% CO_2. The reaction was stopped by adding 100 μL of acetonitrile into the incubation mixture. Samples were then mixed gently and briefly on a plate shaker, transferred completely to a 0.8 mL V-bottom 96-well plate, and centrifuged at 2550*g* for 15 min at room temperature. Each supernatant (150 μL) was transferred to a clean cluster tube, followed by HPLC-MS/MS analysis on a Thermo Electron triple quadrupole system.

Carboxypeptidase Y (EC 3.4.16.1) Assay. The experiment was carried out by dissolving ProTides (3.5 mg) in acetone-d_6 (0.15 mL) followed by addition of 0.30 mL of Trizma buffer (pH 7.6). After recording the control ^{31}P NMR at 25 °C, a previously defrosted carboxypeptidase Y (0.1 mg dissolved in 0.15 mL of Trizma) was added to the sample, which was then immediately submitted to the ^{31}P NMR experiments (at 25 °C). The spectra were recorded with 64 scans every 7 min unless otherwise stated. ^{31}P NMR recorded data were processed and analyzed with the Bruker Topspin 2.1 program.

Cell Culture Conditions. The acute myeloid leukemia (AML) KG1a cell line and the prostate cancer cell line, LNCaP, were maintained in RPMI medium (Invitrogen, Paisley, U.K.) supplemented with 100 units/mL penicillin, 100 μg/mL streptomycin, and 20% fetal calf serum. The colorectal cancer cell lines, HT-29 and HCT-116, and the breast cancer cell line, MDA-MB-231, were maintained in Dulbecco's modified essential medium with high glucose supplemented with 100 units/mL penicillin, 100 μg/mL streptomycin, and 10% fetal calf serum.

Measurement of In Vitro Apoptosis. Cultured cells were harvested by centrifugation and resuspended in 195 μL of calcium-rich buffer. Subsequently, 5 μL of Annexin V was added to the cell suspension and cells were incubated in the dark for 10 min prior to washing. Cells were finally resuspended in 190 μL of calcium-rich buffer together with 10 μL of propidium iodide. Apoptosis was assessed by dual-color immunofluorescent flow cytometry[48] as described previously. Subsequently LC_{50} values (the doses required to kill 50% of the cells in culture) were calculated for each nucleoside analogue and ProTide.

Immunophenotypic Identification of the Cancer Stem Cells. KG1a cells or LNCaP cells were cultured for 72 h in the presence of a wide range of concentrations of each nucleoside analogue and their respective ProTides. Cells were then harvested, and KG1a cells were labeled with anti-CD34 (FITC) and anti-CD38 (PE) and LNCaP cells were labeled with anti-CD44 (APC) and anti-CD133 (Alexa

https://doi.org/10.1021/acs.jmedchem.0c02194
J. Med. Chem. 2021, 64, 8179−8193

488). The subpopulations expressing a cancer stem cell (CSC) phenotype were subsequently identified and were expressed as a percentage of all viable cells left in the culture. The percentages of stem cells remaining were then plotted on a dose−response graph, and the proportion of cancer stem cells was compared across the various concentrations of ProTides and their respective parental nucleoside in order to determine if they preferentially target cancer stem cells.

Cell Sorting. KG1a cells were cultured until confluent in order to generate 10^8 cells. Subsequently, 5×10^6 of $CD34^+/CD38^-$ LSCs and $CD34^+/CD38^+$ bulk tumor cells were purified by high-speed cell sorting using a FACS Melody cell sorter (Becton Dickenson) and were placed back into culture prior to the addition of 1 μM gemcitabine or the ProTide NUC-1031_mix.

Mass Spectrometry Assessment of Intracellular Nucleoside/ProTide. Defined concentrations of nucleoside were run through the mass spectrometer in order to construct a standard curve (Figure 6A). This was used to quantify the levels of nucleoside/ProTide triphosphate in each of the samples provided. KG1a cells (5×10^6), cultured in DMEM + 10% FCS, were exposed to 1 μM of gemcitabine or NUC-1031_mix for 1 h prior to harvesting by centrifugation. Cells were then FACS sorted into LSC (CD34+/CD38-) and bulk tumor cell fractions (CD34+/CD38+). Purified cells were then pelleted prior to lysis and mass spectrometry analysis for intracellular triphosphate content of gemcitabine or NUC-1031.

Immunopheotypic Expression of ABCB1 and ABCG2. KG1a cells were harvested from culture and labeled with anti-CD34 (FITC) and anti-CD38 (PE) to identify the LSC and bulk tumor fractions. In addition, they were labeled with anti-ABCB1 (Alexa 647) and anti-ABCG2 (APC). Subsequently, the LSC and bulk tumor fractions were gated and the expression levels of the two ABC transporters were quantified using mean fluorescence intensity values.

Transcription of ABC Transporter Genes. A volume of 1 mL of TRIzol was added to each pellet of 2×10^5 harvested bulk tumor or LSC cells. A volume of 200 μL of chloroform was added and centrifuged at 8000*g* for 15 min at 4 °C. The aqueous layer was gently removed and added to an equal volume of 70% ethanol. A volume of 700 μL of the sample was then added to an RNeasy spin column, and the RNeasy Mini Kit protocol was followed. The elution step used 50 μL of RNase-free water, and RNA quantification was assessed using a Nanodrop:1000 spectrophotometer. Duplicate 1 μL samples were evaluated, and the RNA concentration, A260/280 ratio, and A260/A230 ratios were obtained. Aliquots of 0.5 μg of RNA were then added to 0.5 mL microfuge tubes containing 10 μL of master mix and made up to 20 μL with sterile RNase-free water. Samples were added to the thermal cycler and run as per the kit's protocol. Once the run was complete, 20 μL of newly converted cDNA was diluted 5:1 with sterile DNA and RNase-free water to give a working concentration of 2.5 ng/μL. Samples were stored at −20 °C. The TaqMan Fast Advanced Master Mix kit protocol was followed. Samples were run in triplicate, including a minus RT sample and a minus cDNA sample. Samples were run on a 96-well plate with a running volume 10 μL per well. This was composed of 2.5 μL of thawed cDNA, 0.5 μL of forward and reverse primers (ABC transporter gene or GAPDH as a housekeeping control; see Table S1, Supporting Information), 5 μL of TaqMan master mix, and 2 μL of RNase-free water. Samples were run on a ViiA7 real-time PCR system using the TaqMan FAST program. Results were analyzed using the Thermo Fisher Cloud software using the Relative Quantification qPCR application.

Statistical Analysis. The data obtained in these experiments were evaluated using one-way ANOVA. All data was confirmed as Gaussian or a Gaussian approximation using the omnibus K2 test. LC_{50} values were calculated from the nonlinear regression and line of best-fit analysis of the sigmoidal dose−response curves. Values are shown as mean ± SEM from each replicate data set. All statistical analyses were performed using Graphpad Prism 6.0 software (GraphPad Software Inc., San Diego, CA).

Crystal Structure Determination. Single-crystal XRD data were collected on an Agilent SuperNova Dual Atlas diffractometer with a mirror monochromator using Cu (λ = 1.5418 Å) . Crystal structures were solved and refined using SHELX (see Table S2, Supporting Information).[49,50] Geometric restraints were applied during refinement of orientationally disordered components. Non-hydrogen atoms were refined with anisotropic displacement parameters. Hydrogen atoms were inserted in idealized positions, and a riding model was used.

General Methods. All solvents and reagents were used as obtained from commercial sources unless otherwise indicated. All reactions were performed under a nitrogen atmosphere. The ^1H and ^{13}C NMR spectra were recorded on a Varian spectrometer operating at 500 MHz for ^1H and 125 MHz for ^{13}C. Deuterated chloroform was used as the solvent for NMR experiments, unless otherwise stated. ^1H chemical shifts values (δ) are referenced to the residual nondeuterated components of the NMR solvents (δ = 7.26 ppm for $CHCl_3$, etc.). The ^{13}C chemical shifts (δ) are referenced to $CDCl_3$ (central peak, δ = 77.0 ppm). Fluorine chemical shifts are referenced to $CFCl_3$. Mass spectra were measured in positive mode electrospray ionization (ESI). Thin layer chromatography (TLC) was performed on silica gel 60 F254 plastic sheets. Column chromatography was performed using silica gel (35−75 mesh). Purity of prepared compounds was determined by high-pressure liquid chromatography-ultraviolet (HPLC-UV) analysis (Thermo HPLC connected with UV detector). The purity of all final compounds was determined to be >95% by reversed phase-high-pressure liquid chromatography (RP-HPLC) using the eluents water (eluent A), acetonitrile (eluent B), and the following conditions: Varian Pursuit XS, 4.6 mm × 150 mm, 5.0 μm, 1.0 mL/min, gradient 30 min 10% → 100% eluent B in eluent A (method 1). The purity of the intermediates was >90%, unless otherwise stated.

*General Procedure 1 for the Preparation of 3′,5′-TBDMS Protected FUDR (**3**) and of 3′,5′-TBDMS Protected Gemcitabine (**4**).* TBDMSCl (2.2 equiv) was added to a stirred solution of nucleoside (1.0 equiv), imidazole (5.0 equiv), and DMAP (0.3 equiv) in DMF (10 mL) at 0 °C, and the mixture was allowed to warm to 25 °C and stirred for 1 h. The reaction was quenched with saturated aqueous solution of ammonium chloride, followed by extraction with EtOAc (3 × 5 mL). The combined organic layers were dried over Na_2SO_4, and the solvent was removed under vacuum to give a crude product as an oil used for the next step without further purification.

2′-Deoxy-5-fluoro-3′,5′-bis(*O-tert*-butyldimethylsilyl-uridine (**3**) was obtained from FUDR (2.0 g, 8.10 mmol), imidazole (40.62 mmol, 2.76 g), DMAP (2.43 mmol, 0.297 g), and TBDMSCl (17.87 mmol, 2.70 g) in DMF (15 mL) as an oil. Yield, 83% (3.20 g). ^1H NMR (500 MHz, CD_3OD): δ_H 8.02 (d, J = 6.5 Hz, 1H, *H*-6), 6.30 (t, J = 7.50, 1H, *H*-1′), 4.40 (q, J = 3.5 Hz, 1H, *H*-3′), 3.97−3.86 (m, 2H, *H*-4′, *H*-5′), 3.74 (dd, 1H, J = 12.0, 3.5 Hz, *H*-5′), 2.40−2.31 (m, 1H, *H*-2′), 2.10−2.00 (m, 1H, *H*-2′), 0.93, 0.92 (2*s*, 18H, $C(CH_3)_3$), 0.12, 0.11 (2*s*, 12H, $Si(CH_3)_2$). ^{13}C NMR (125 MHz, $CDCl_3$): δ_C 157.23 (d, $^2J_{C-F}$ = 26.0 Hz, *C*-4), 149.17 (*C*-2), 141.54 (d, $^1J_{C-F}$ = 235.0 Hz, *C*-5), 124.12 (d, $^2J_{C-F}$ = 33.7 Hz, *C*-6), 87.98 (*C*-4′), 85.46 (*C*-1′), 71.38 (*C*-3′), 62.58 (*C*-5′), 41.73 (*C*-2′), 25.65 ($C(CH_3)_3$), 18.37, 18.06 ($C(CH_3)_3$), −4.67, −4.93 ($Si(CH_3)_2$).

2′-Deoxy-2′,2′-difluoro-3′,5′-bis(*O-tert*-butyldimethylsilyl-D-cytidine (**4**) was obtained from gemcitabine (2.0 g, 7.59 mmol), imidazole (2.58 g, 37.95 mmol), DMAP (0.278 g, 2.27 mmol), and TBDMSCl (2.52 g, 16.69 mmol) in DMF (15 mL) as an oil. Yield 82% (3.05 g). ^1H NMR (500 MHz, CD_3OD): δ_H 7.74 (d, J = 8.0 Hz, 1H, *H*-6), 6.27 (dd, J_{H-F} = 9.50, 5.50 Hz, 1H, *H*-1′), 5.77 (d, J = 7.5 Hz, 1H, *H*-5), 4.38−4.28 (m, 1H, *H*-3′), 4.02 (dd, 1H, J = 11.5, 3.5 Hz, *H*-5′a), 3.92−3.88 (m, 1H, *H*-4′), 3.80 (dd, 1H, J = 2.0, 11.5 Hz, *H*-5′b), 0.93, 0.92 (2*s*, 18H, $C(CH_3)_3$), 0.12, 0.11 (2*s*, 12H, $Si(CH_3)_2$).

*2′-Deoxy-5-fluoro-3′-(O-tert-butyldimethylsilyl-uridine (**5**).* CSA (6.74 mmol, 1.56 g) was added to 2′-deoxy-5-fluoro-3′,5′-bis(*O-tert*-butyldimethylsilyl-uridine (**3**) (6.74 mmol, 3.20 g) dissolved in MeOH (15 mL), at 0 °C and the reaction mixture was stirred under an argon atmosphere for 10 min. After the reaction was completed, the solvent was removed under reduced pressure to yield the crude residue that was purified by silica gel column chromatography with a gradient of MeOH (1% to 10%) in DCM as an eluent to afford **5** as a

https://doi.org/10.1021/acs.jmedchem.0c02194
J. Med. Chem. 2021, 64, 8179−8193

white solid. Yield, 60% (1.45 g). ^{1}H NMR (500 MHz, DMSO-d_6): δ_H 8.22 (d, J_{H-F} = 8.0 Hz, 1H, *H*-6), 6.25 (td, *J* = 7.5, 2.0 Hz 1H, *H*-1′), 5.20 (t, *J* = 3.0 Hz, 1H, 5′-O*H*), 4.53 (q, *J* = 3.5 Hz, 1H, *H*-3′), 3.92 (qr, *J* = 3.5 Hz, 1H, *H*-4′), 3.80 (dd, *J* = 12.0, 3.5 Hz, 1H, *H*-5′), 3.73 (dd, *J* = 12.0, 3.5 Hz, 1H, *H*-5′), 2.26−2.21 (m, 2H, *H*-2′), 0.94 (s, 9H, C(CH_3)$_3$), 0.15 (s, 6H, Si(CH_3)$_2$). ^{13}C NMR (125 MHz, CD_3OD): δ_C 159.46 (d,$^2J_{C-F}$ = 26.2 Hz, *C*-4), 150.83 (*C*-2), 141.87 (d,$^1J_{C-F}$ = 231.0 Hz, *C*-5), 126.24 (d,$^2J_{C-F}$ = 35.0 Hz, *C*-6), 89.58 (*C*-4′), 86.83 (*C*-1′), 73.46 (*C*-3′), 62.38 (*C*-5′), 41.99 (*C*-2′), 26.41 (C(CH_3)$_3$), 18.84 (C(CH_3)$_3$), −4.65 (d,$^1J_{C-Si}$ = 18.7 Hz, (Si(CH_3)$_2$). MS (MSI+): *m*/*z* calcd for $C_{15}H_{25}FN_2O_5Si$: 360.45 [M]$^+$; found 383.149 [M + Na]$^+$.

*2′-Deoxy-2′,2′-difluoro-3′-(O-tert-butyldimethylsilyl)-D-cytidine (**6**).* A solution of trichloroacetic acid (113.88 mmol, 11.42 mmol) in 8.7 mL of water was added to a solution of compound **4** (2.0 g, 4.06 mmol) in THF (38 mL) at 0 °C. The reaction mixture was stirred for 2 h at rt, and then the reaction solution was neutralized with solid $NaHCO_3$ until evolution of gas was finished. Next, 100 mL of water was added to the reaction mixture, followed by extraction with EtOAc (3 × 50 mL). The volatiles were concentrated under reduced pressure to afford the title compound **6** as a white solid. Yield, 82% (1.25 g). ^{1}H NMR (500 MHz, DMSO-d_6): δ_H 7.54 (d, *J* = 7.5 Hz, 1H, *H*-6), 7.55, 7.53 (2 × bs, 2H, NH_2), 6.03 (t, J_{H-F} = 8.0 Hz, 1H, *H*-1′), 5.68 (d, *J* = 7.5 Hz, 1H, *H*-5), 5.15 (bs, 1H, O*H*-5′), 4.25−4.18 (m, 1H, *H*-3′), 3.71−3.64 (m, 2H, *H*-4′, *H*-5′a), 3.46 (dd, *J* = 12.5, 3.5 Hz, 1H, *H*-5′b), 0.77 (s, 9H, C(CH_3)$_3$), 0.00, −0.02 (2*s*, 6H, Si(CH_3)$_2$). ^{13}C NMR (125 MHz, CD_3OD): δ_C 165.99 (*C*−NH_2), 156.16 (C═O base), 140.43 (*C*H−base), 122.61 (t,$^1J_{C-F}$ = 256 Hz, CF_2), 95.16 (*C*H−base), 84.35 (t,$^2J_{C-F}$ = 31.7 Hz, *C*-1′), 80.67 (t,$^3J_{C-F}$ = 4.0 Hz, *C*-4′), 68.39 (t,$^2J_{C-F}$ = 22.8 Hz, *C*-3′), 60.35 (*C*-5′), 25.09, 24.92 (C(CH_3)$_3$), 17.92 (*C*(CH_3)$_3$), −6.65 (d,$^1J_{C-Si}$ = 12.9 Hz, Si(CH_3)$_2$).

General Procedure 2 for a Preparation of 3′-TBDMS-Protected ProTides. *tert*-BuMgCl (1.0 M solution in THF, 1.2 equiv) was added to a solution of 3′-O-(*tert*-butyldimethylsilyl)-protected nucleoside (1.0 equiv) in dry THF (10 mL), in one portion followed by addition of an appropriate phosphorochloridate (2.0 equiv) dissolved in anhydrous THF (3 mL). The reaction mixture was stirred for 16 h and then evaporated under reduced pressure to give a crude residue that was purified either by silica gel column chromatography, eluting with a gradient of MeOH (0−2%) in DCM or with a gradient of MeOH (3−6%) in a mixture of EtOAc (15%) and DCM as an eluent, followed by TLC preparative purification unless stated otherwise to afford 3′-TBDMS-protected ProTides as single diastereoisomers.

2′-Deoxy-5-fluoro-3′-*O*-*tert*-butyl-dimethylsilyl-D-uridine-5′-*O*-[naphthyl-(benzyloxy-L-alaninyl)] phosphate (**7**) was prepared according to general procedure 2 from 2′-deoxy-5-fluoro-3′-(*O*-*tert*-butyldimethylsilyl-uridine (**5**) (2.77 mmol, 1.0 g) and L-Ala-OBn-ONaph phosphorochloridate[10] (5.55 mmol, 2.24 g), (3.33 mmol, 3.33 mL) in THF (15 mL). The crude mixture was purified by silica column chromatography with a slow gradient of MeOH (0−2%) in DCM as an eluent to give the fast eluting isomer A (**7a**,S_P) or (**7b**,R_P) and the slow eluting isomer B (**7a**, S_P) or (**7b**,R_P).

2′-Deoxy-5-fluoro-3′-*O*-(*tert*-butyl-dimethylsilyl)-D-uridine-5′-*O*-[naphthyl-(benzyloxy-L-alaninyl)] phosphate (**7_Isomer A**) was the fast eluting fraction obtained as a white solid. Yield, 9% (0.19 g) ^{31}P NMR (202 MHz, CD_3OD): δ_P 4.64. ^{1}H NMR (500 MHz, CD_3OD): δ_H 8.15 (d, *J* = 8.0 Hz, 1H, Ar-*H*), 7.89 (d, *J* = 8.0 Hz, 1H, *H*-Ar), 7.73 (d, J_{H-F} = 8.0 Hz, 1H, *H*-6), 7.65 (d, *J* = 6.5 Hz, 1H, Ar-*H*), 7.54−7.50 (m, 3H, Ar-*H*), 7.43. (t, *J* = 8.0 Hz, 1H, Ar-*H*), 7.34−7.28 (m, 5H, Ar-*H*), 6.08 (t, *J* = 6.5 Hz 1H, *H*-1′), 5.06 (ABq, J_{A-B} = 12.0 Hz, 2H, OCH_2Ph), 4.30−4.28 (m, 3H, 2 × *H*-5′, *H*-3′), 4.15−4.11 (m, 1H, *CH*CH_3), 3.97−3.95 (m, 1H, *H*-4′), 1.96 (ddd, *J* = 13.5, 5.5, 2.5 Hz, 1H, *H*-2′), 1.55−1.50 (m, 1H, *H*-2′), 1.38 (d, *J* = 7.0 Hz, 3H, CH*CH*$_3$), 0.89 (s, 9H, C(CH_3)$_3$), 0.01 (d,$^2J_{Si-H}$ = 5.5 Hz, 6H, Si(CH_3)$_2$). MS (MSI$^+$): *m*/*z* calcd for $C_{35}H_{43}FN_3O_9PSi$: 727.78 [M]$^+$; found 750.25 [M + Na]$^+$.

2′-Deoxy-5-fluoro-3′-*O*-(*tert*-butyl-dimethylsilyl)-D-uridine-5′-*O*-[naphthyl-(benzyloxy-L-alaninyl)] phosphate (**7_Isomer B**) was the slow eluting fraction obtained as a white solid. Yield, 12% (0.25 g). ^{31}P NMR (202 MHz, CD_3OD): δ_P 4.28. ^{1}H NMR (500 MHz, CD_3OD): δ_H 8.17−8.14 (m, 1H, *H*-Ar), 7.88−7.86 (m, 1H, *H*-Ar), 7.70 (d, J_{H-F} = 6.5 Hz, 1H, *H*-6), 7.60 (d, *J* = 8.5 Hz, 1H, *H*-Ar), 7.54−7.50 (m, 3H, *H*-Ar), 7.37 (t, *J* = 8.0 Hz, 1H, *H*-Ar), 7.33−7.27 (m, 5H, *H*-Ar), 6.06 (t, *J* = 7.5 Hz 1H, *H*-1′), 5.06 (apparent s, 2H, OCH_2Ph), 4.32−4.27 (m, 2H, *H*-3′, *H*-5′), 4.23−4.19 (m, 1H, *H*-5′), 4.15−4.11 (m, 1H, *CH*CH_3), 3.99−3.97 (m, 1H, *H*-4′), 1.98 (ddd, *J* = 13.5, 5.5, 2.5 Hz, 1H, *H*-2′), 1.59−1.54 (m, 1H, *H*-2′), 1.38 (d, *J* = 7.0 Hz, 3H, CH*CH*$_3$), 0.87 (s, 9H, C(CH_3)$_3$), 0.04 (d,$^2J_{Si-H}$ = 5.5 Hz, 6H, Si(CH_3)$_2$). ^{13}C NMR (125 MHz, CD_3OD): δ_C 173.08 (d,$^3J_{C-P}$ = 4.8 Hz, C═O, ester), 157.95 (d,$^2J_{C-F}$ = 26.2 Hz, *C*-4), 149.12 (*C*-2), 146.41 (d,$^2J_{C-P}$ = 7.8 Hz, OC-Naph), 140.32 (d,$^1J_{C-F}$ = 232.0 Hz, *C*-5), 135.74, 134.90 (*C*-Ar), 128.19, 127.96, 127.89, 127.60, 126.51 (*C*H−Ar), 126.47, 126.42 (*C*-Ar), 126.20, 125.17, 124.84 (CH−Ar), 124.28 (d,$^2J_{C-F}$ = 34.1 Hz, *C*-6), 121.20 (CH-Ar), 115.17 (d,$^3J_{C-P}$ = 3.2 Hz, CH−Ar), 85.77 (d,$^3J_{C-P}$ = 7.7 Hz, *C*-4′), 85.55 (*C*-1′), 72.10 (*C*-3′), 66.63 (OCH_2Ph), 66.11 (d,$^2J_{C-P}$ = 5.5 Hz, *C*-5′), 50.46 (*CH*CH_3), 39.80 (*C*-2′), 24.81 (C(CH_3)$_3$), 18.99 (d,$^3J_{C-P}$ = 6.9 Hz, CHCH_3), 17.34 (*C*(CH_3)$_3$), −6.06 (d,$^1J_{C-Si}$ = 14.2 Hz, Si(CH_3)$_2$). MS (MSI+): *m*/*z* calcd for $C_{35}H_{43}FN_3O_9PSi$: 727.78 [M]$^+$; found 750.25 [M + Na]$^+$.

2′-Deoxy-2′,2′-difluoro-3′-*O*-(*tert*-butyl-dimethylsilyl)-D-cytidine-5′-*O*-[phenyl(benzyloxy-L-alaninyl)] phosphate (**8**) was obtained from 3′-*O*-(*tert*-butyldimethylsilyl)-gemcitabine **6** (2.66 mmol, 1.0 g) in dry THF (14 mL), *tert*-BuMgCl (2.90 mmol, 2.9 mL), and L-Ala-OBn-OPh phosphorochloridate[9] (3.97 mmol, 1.40 g) dissolved in anhydrous THF (5 mL). The reaction mixture was stirred for 16 h and then evaporated in vacuum to give a crude residue that was purified by column chromatography on silica gel, eluting with a gradient of DCM/EtOAc/MeOH (82%/15%/3%) to (79%/15%/6%) to afford **8b** as the fast eluting fraction and **8a** as the slow eluting fraction.

2′-Deoxy-2′,2′-difluoro-3′-*tert*-butylsilyl-D-cytidine-5′-*O*-[phenyl-(benzyloxy-L-alaninyl)] phosphate (**8a**) was the slow eluting fraction obtained as a white solid. Yield, 30% (0.55 g). ^{31}P NMR (202 MHz, CD_3OD): δ_P 3.56. ^{1}H NMR (500 MHz, CD_3OD): δ_H 7.40 (d, *J* = 7.5 Hz, 1H, *H*-6), 7.22−7.16 (m, 7H, Ar-*H*), 7.09−7.04 (m, 3H, Ar-*H*), 6.07 (t, J_{H-F} = 8.5 Hz 1H, *H*-1′), 5.71 (d, *J* = 7.5 Hz, 1H, *H*-5), 5.00, 4.96 (AB q, J_{AB} = 12.0, 9.0 Hz, 2H, OCH_2Ph), 4.31−4.27 (m, 1H, *H*-3′), 4.22−4.16 (m, 1H, *H*-4′), 4.13−4.08 (m, 1H, *H*-5′), 3.89−3.83 (m, 2H, *H*-5′, *CH*CH_3), 1.23 (dd, *J* = 7.0, 1.5 Hz, 3H, CH*CH*$_3$), 0.78 (s, 9H, C(CH_3)$_3$), 0.0 (s, 6H, Si(CH_3)$_2$). ^{13}C NMR (125 MHz, CD_3OD): δ_C 173.07 (d,$^3J_{C-P}$ = 5.3 Hz, *C*═O, ester), 166.26 (*C*-NH_2), 156.28 (*C*═O base), 150.68 (d,$^2J_{C-P}$ = 3.3 Hz, *C*-Ar), 141.11 (*C*H-base), 135.79 (*C*-Ar), 129.50, 128.22, 127.98, 127.88, 124.94 (*C*H-Ar), 122.83 (d,$^1J_{C-F}$ = 258 Hz, CF_2), 120.02, 119.98 (CH-Ar), 95.28 (CH-base), 79.39 (broad signal, *C*-1′), 79.35 (*C*-4′), 71.05 (apparent t,$^2J_{C-F}$ = 26.1 Hz, *C*-3′), 66.60 (OCH_2Ph), 64.02 (d,$^2J_{C-P}$ = 4.9 Hz, *C*-5′), 50.29 (*CH*CH_3), 24.63 (C(CH_3)$_3$), 19.02 (d,$^3J_{C-P}$ = 6.8 Hz, CH*CH*$_3$), 17.47 (*C*(CH_3)$_3$), −6.20 (d,$^1J_{C-Si}$ = 29.1 Hz, Si(CH_3)$_2$). MS (ESI+) *m*/*z* calcd for $C_{31}H_{41}F_2N_4O_8PSi$: 694.73 [M$^+$]; found 717.45 [M + Na] $^+$.

2′-Deoxy-2′,2′-difluoro-3′-*tert*-butylsilyl-D-cytidine-5′-*O*-[phenyl-(benzyloxy-L-alaninyl)] phosphate (**8b**), the fast eluting fraction, was obtained as a white solid. Yield, 25% (0.45 g). ^{31}P NMR (202 MHz, CD_3OD): δ_P 3.71. ^{1}H NMR (500 MHz, CD_3OD): δ_H 7.45 (d, *J* = 7.5 Hz, 1H, *H*-6), 7.24−7.18 (m, 7H, Ar-*H*), 7.09−7.07 (m, 3H, Ar-*H*), 6.12 (t, J_{H-F} = 8.5 Hz 1H, *H*-1′), 5.78 (d, *J* = 7.5 Hz, 1H, *H*-5), 5.04, 5.01 (AB q, J_{AB} = 12.5, 3.0 Hz, 2H, OCH_2Ph), 4.39−4.36 (m, 1H, *H*-3′), 4.23−4.13 (m, 2H, *H*-5′, *H*-4′), 3.93−3.87 (m, 2H, *H*-5′, *CH*CH_3), 1.24 (dd, *J* = 7.0, 1.5 Hz, 3H, CH*CH*$_3$), 0.80 (s, 9H, C(CH_3)$_3$), 0.0 (s, 6H, Si(CH_3)$_2$). ^{13}C NMR (125 MHz, CD_3OD): δ_C 173.35 (d,$^3J_{C-P}$ = 4.2 Hz, *C*═O, ester), 166.26 (*C*-NH_2), 156.26 (*C*═O base), 150.63 (d,$^2J_{C-P}$ = 2.4 Hz, *C*-Ar), 140.89 (*C*H-base), 135.82 (*C*-Ar), 129.47, 128.21, 127.98, 127.92, 125.57 (*C*H−Ar), 123.90 (d,$^1J_{C-F}$ = 266 Hz, CF_2), 120.11, 120.07 (*C*H-Ar), 95.38 (*C*H-base), 79.24 (broad signal, *C*-1′), 75.23 (broad signal, *C*-4′), 70.94 (broad signal, *C*-3′), 66.59 (OCH_2Ph), 63.59 (d,$^2J_{C-P}$ = 5.0 Hz, *C*-5′), 50.47 (*CH*CH_3), 24.62 (C(CH_3)$_3$), 18.82 (d,$^3J_{C-P}$ = 7.7 Hz, CHCH_3), 17.47 (*C*(CH_3)$_3$), −6.21 (d,$^1J_{C-Si}$ = 28.1 Hz, Si(CH_3)$_2$).

https://doi.org/10.1021/acs.jmedchem.0c02194
J. Med. Chem. 2021, 64, 8179−8193

MS (ESI+) m/z calcd for $C_{31}H_{41}F_2N_4O_8PSi$: 694.73 [M^+]; found 717.45 [M + Na] $^+$.

*General Procedure 3 for the 3′-Desilylation of 3′-TBDMS-Protected ProTides **7a**, **7b** and **8a**, **8b**.* The separated diastereoisomer of 3′-TBDMS-protected ProTide (**7a**, **7b**, **8a**, and **8b**) was treated with a mixture of THF/TFA/DCM (4:1:1) at 0 °C. The resulting reaction mixture was stirred at 0 °C for 2 h and then at room temperature for 12 h. After the reaction was completed, the solvents were evaporated, and the residue was purified on silica gel with a gradient of MeOH (2−8%) in DCM as an eluent.

2′-Deoxy-5-fluoro-D-uridine-5′-*O*-[naphthyl-(benzyloxy-L-alaninyl)] phosphate (**9a** or **9b**, NUC-3373_IsoA) was obtained from the fast eluting **7_isomer A** (**7a** or **7b**) (0.19 g, 0.26 mmol) as a white solid. Yield, 75% (0.12 g). ^{31}P NMR (202 MHz, CD_3OD): δ_P 4.60. ^{19}F NMR (470 MHz, CD_3OD): δ_F − 167.05. ^{1}H NMR (500 MHz, CD_3OD): δ_H 8.14 (dd, J = 8.5, 2.0 Hz, 1H, Ar-*H*), 7.87 (d, J = 7.0 Hz, 1H, *H*-Ar), 7.72 (apparent s, 1H, Ar-*H*), 7.69 (d, J_{H-F} = 6.5 Hz, 1H, *H*-6), 7.54−7.49 (m, 3H, Ar-*H*), 7.42 (t, J = 8.0 Hz, 1H, Ar-*H*), 7.34−7.28 (m, 5H, Ar-*H*), 6.14 (t, J = 6.0 Hz 1H, *H*-1′), 5.10 (ABq, J_{A-B} = 12.5 Hz, 2H, OCH_2Ph), 4.35−4.33 (m, 2H, *H*-3′, *H*-5′), 4.30−4.28 (m, 1H, *H*-5′), 4.14−4.08 (m, 1H, $CHCH_3$), 4.07−4.05 (m, 1H, *H*-4′), 2.11 (ddd, J = 14.0, 6.0, 3.0 Hz, 1H, *H*-2′), 1.73−1.68 (m, 1H, *H*-2′), 1.33 (dd, J = 7.5, 1.5 Hz, 3H, $CHCH_3$). ^{13}C NMR (125 MHz, CD_3OD): δ_C 174.92 (d,$^3J_{C-P}$ = 3.9 Hz, *C*═O, ester), 159.27 (d,$^2J_{C-F}$ = 25.9 Hz, *C*-4), 150.52 (*C*-2), 147.90 (d,$^2J_{C-P}$ = 7.3 Hz, OC-Naph), 141.73 (d,$^1J_{C-F}$ = 232.3 Hz, *C*-5), 137.19, 136.29 (*C*-Ar), 129.59, 129.36, 128.91, 127.90 (*C*H-Ar), 127.85, 127.80 (*C*-Ar), 127.60 (*C*H-Ar), 126.50 (d,$^3J_{C-P}$ = 1.4 Hz, *C*H-Naph), 126.18 (*C*H-Ar), 125.53 (d,$^2J_{C-F}$ = 34.0 Hz, *C*-6), 122.64 (*C*H-Ar), 116.30 (d,$^3J_{C-P}$ = 3.12 Hz, *C*H-Ar), 86.93 (*C*-1′), 86.88 (d,$^3J_{C-P}$ = 8.0 Hz, *C*-4′), 72.18 (*C*-3′), 68.10 (OCH_2Ph), 67.86 (d,$^2J_{C-P}$ = 5.2 Hz, *C*-5′), 51.96 ($CHCH_3$), 40.84 (*C*-2′), 20.24 (d,$^3J_{C-P}$ = 7.5 Hz, $CHCH_3$). MS (MSI+): m/z calcd for $C_{29}H_{29}FN_3O_9P$: 613.53 [M^+]; found 636.15 [M + Na]$^+$. Reverse HPLC eluting with (H_2O/AcCN from 100/0 to 0/100) in 30 min, t_R 16.61 min.

2′-Deoxy-5-fluoro-D-uridine-5′-*O*-[naphthyl-(benzyloxy-L-alaninyl)] phosphate (**9a** or **9b**, NUC-3373_IsoB) was obtained from the slow eluting **7_isomer B** (**7a** or **7b**) (0.24 g, 0.36 mmol) (0.19 g, 0.26 mmol) as a white solid. Yield, 75% (0.15 g). ^{31}P NMR (202 MHz, CD_3OD): δ_P 4.26. ^{19}F NMR (470 MHz, CD_3OD): δ_F −167.31. ^{1}H NMR (500 MHz, CD_3OD): δ_H 8.17−8.14 (m, 1H, Ar-*H*), 7.90−7.87 (m, 1H, Ar-*H*), 7.72 (apparent s, 1H, Ar-*H*), 7.69 (d, J_{H-F} = 6.0 Hz, 1H, *H*-6), 7.54−7.48 (m, 3H, Ar-*H*), 7.38 (t, J = 8.0 Hz, 1H, Ar-*H*), 7.34−7.28 (m, 5H, Ar-*H*), 6.10 (t, J = 6.0 Hz 1H, *H*-1′), 5.12 (s, 2H, OCH_2Ph), 4.36−4.25 (m, 3H, *H*-3′, 2 × *H*-5′), 4.14−4.08 (m, 1H, $CHCH_3$), 4.05 (apparent q, J = 2.5 Hz, 1H, *H*-4′), 2.14 (ddd, J = 14.0, 6.0, 3.0 Hz, 1H, *H*-2′), 1.75−1.69 (m, 1H, *H*-2′), 1.36 (dd, J = 7.0, 0.5 Hz, 3H, $CHCH_3$). ^{13}C NMR (125 MHz, CD_3OD): δ_C 174.57 (d,$^3J_{C-P}$ = 4.5 Hz, *C*═O, ester), 159.38 (d,$^2J_{C-F}$ = 26.0 Hz, *C*-4), 150.48 (*C*-2), 147.80 (d,$^2J_{C-P}$ = 7.3 Hz, OC-Naph), 141.67 (d,$^1J_{C-F}$ = 232.0 Hz, *C*-5), 137.15, 136.27 (*C*-Ar), 129.63, 129.40, 129.36, 128.97, 127.89 (*C*H-Ar), 127.86, 127.81 (*C*-Ar), 127.59 (*C*H-Ar), 126.56 (d,$^3J_{C-P}$ = 1.4 Hz, *C*H-Naph), 126.22 (*C*H-Ar), 125.62 (d,$^2J_{C-F}$ = 34.1 Hz, *C*-6), 122.63 (*C*H-Ar), 116.56 (d,$^3J_{C-P}$ = 3.0 Hz, *C*H-Ar), 86.98 (*C*-1′), 86.68 (d,$^3J_{C-P}$ = 7.6 Hz, *C*-4′), 72.02 (*C*-3′), 68.08 (OCH_2Ph), 67.85 (d,$^2J_{C-P}$ = 5.5 Hz, *C*-5′), 51.84 ($CHCH_3$), 40.90 (*C*-2′), 20.44 (d,$^3J_{C-P}$ = 6.7 Hz, $CHCH_3$). MS (MSI+): m/z calcd for $C_{29}H_{29}FN_3O_9P$: 613.53 [M^+]; found 636.15 [M + Na]$^+$. Reverse HPLC eluting with (H_2O/AcCN from 100/0 to 0/100) in 30 min, t_R 16.03 min.

2′-Deoxy-2′,2′-difluoro-D-cytidine-5′-*O*-[phenyl(benzyloxy-L-alaninyl)] phosphate (**10a**, NUC-1031_S_P) obtained from **8a** (0.55 g, 0.79 mmol) as a white, crystalline solid. Yield, 76% (0.35 g). ^{31}P NMR (202 MHz, CD_3OD): δ_P 3.66. ^{19}F NMR (470 MHz, CD_3OD): δ_F −118.0 (d, J = 241 Hz, *F*), −120.24 (broad d, J = 241 Hz, *F*). ^{1}H NMR (500 MHz, CD_3OD): δ_H 7.58 (d, J = 7.5 Hz, 1H, *H*-6), 7.38−7.32 (m, 7H, Ar-*H*), 7.26−7.20 (m, 3H, Ar-*H*), 6.24 (t, J = 7.5 Hz, 1H, *H*-1′), 5.84 (d, J = 7.5 Hz, 1H, *H*-5), 5.20 (AB q, J_{AB} = 12.0, 7.2 Hz, 2H, OCH_2Ph), 4.46−4.43 (m, 1H, *H*-5′), 4.36−4.31 (m, 1H, *H*-5′), 4.25−4.19 (m, 1H, *H*-3′), 4.07−4.00 (m, 2H, *H*-4′, $CHCH_3$), 1.38 (d, J = 7.2 Hz, 3H, $CHCH_3$). ^{13}C NMR (125 MHz, CD_3OD): δ_C 174.61 (d,$^3J_{C-P}$ = 5.0 Hz, *C*═O, ester), 167.64 (*C*-NH_2), 157.74 (*C*═O base), 152.10 (d,$^2J_{C-P}$ = 7.0 Hz, *C*-Ar), 142.41 (*C*H-base), 137.22 (*C*-Ar), 130.91, 129.64, 129.40, 129.33, 126.33 (*C*H-Ar), 124.51 (d,$^1J_{C-F}$ = 257 Hz, CF_2), 121.47, 121.44 (*C*H−Ar), 96.67 (*C*H-base), 86.08 (broad signal, *C*-1′), 80.32 (*C*-4′), 71.27 (apparent t,$^2J_{C-F}$ = 23.7 Hz, *C*-3′), 68.04 (OCH_2Ph), 65.74 (d,$^2J_{C-P}$ = 5.30 Hz, *C*-5′), 51.67 ($CHCH_3$), 20.44 (d,$^3J_{C-P}$ = 6.25 Hz, $CHCH_3$). (ESI+) m/z, found: (M + Na^+) 603.14. $C_{25}H_{27}F_2N_4O_8NaP$ required: (M^+) 580.47. Reverse HPLC, eluting with H_2O/MeOH from 100/0 to 0/100 in 35 min, t_R = 18.32 min.

2′-Deoxy-2′,2′-difluoro-D-cytidine-5′-*O*-[phenyl(benzyloxy-L-alaninyl)] phosphate (**10b**, NUC-1031_R_P) was obtained from **8b** (0.45 g, 0.65 mmol) as a white, crystalline solid. Yield, 78% (0.29 g). ^{31}P NMR (202 MHz, CD_3OD): δ_P 3.83. ^{19}F NMR (470 MHz, CD_3OD): δ_F −118.3 (d, J = 241 Hz, *F*), −120.38 (broad d, J = 241 Hz, *F*). ^{1}H NMR (500 MHz, CD_3OD): δ_H 7.56 (d, J = 7.5 Hz, 1H, *H*-6), 7.38−7.31 (m, 7H, Ar-*H*), 7.23−7.19 (m, 3H, Ar-*H*), 6.26 (t, J = 7.5 Hz, 1H, *H*-1′), 5.88 (d, J = 7.5 Hz, 1H, *H*-5), 5.20 (s, 2H, OCH_2Ph), 4.49−4.46 (m, 1H, *H*-5′), 4.38−4.34 (m, 1H, *H*-5′), 4.23−4.17 (m, 1H, *H*-3′), 4.07−4.01 (m, 2H, *H*-4′, $CHCH_3$), 1.38 (d, J = 7.2 Hz, 3H, $CHCH_3$). ^{13}C NMR (125 MHz, CD_3OD): δ_C 174.65 (d,$^3J_{C-P}$ = 5.0 Hz, C═O, ester), 167.65 (*C*-NH_2), 157.75 (C═O base), 152.10 (d,$^2J_{C-P}$ = 7.0 Hz, *C*-Ar), 142.28 (*C*H-base), 137.50 (*C*-Ar), 130.86, 129.63, 129.40, 129.32, 126.31 (*C*H-Ar), 123.73 (d,$^1J_{C-F}$ = 252 Hz, CF_2), 121.44, 121.40 (*C*H-Ar), 96.67 (*C*H-base), 85.90 (broad signal, *C*-1′), 80.27 (*C*-4′), 71.02 (apparent t,$^2J_{C-F}$ = 23.7 Hz, *C*-3′), 68.04 (OCH_2Ph), 65.52 (d,$^2J_{C-P}$ = 5.30 Hz, *C*-5′), 51.85 ($CHCH_3$), 20.23 (d,$^3J_{C-P}$ = 7.5 Hz, $CHCH_3$). (ESI+) m/z, found: (M + Na^+) 603.14. $C_{25}H_{27}F_2N_4O_8NaP$ required: (M^+) 580.47. Reverse HPLC, eluting with H_2O/MeOH from 100/0 to 0/100 in 35 min, t_R = 19.15 min.

*General Method for Crystallization of **7_isoB** from the Column Purified Amorphous **7_isoB** Using the Modified Procedure.*[26] The chromatographed fraction containing the compound **7_isoB** (50 mg, 97%) was dissolved in 5 mL of 2-propanol and diluted with hexane until cloudy. The solution was seeded and stirred at room temperature for 5 h. The resulting solid was filtered, washed with hexane (2 × 2 mL), and dried under a high vacuum. The obtained solid was not suitable for single crystal X-ray analysis. Multiple attempts to crystallize **7_isoA**, **7_isoB**, **9_isoA**, and **9_isoB** by slow evaporation of MeOH, 2-propanol, $CHCl_3$, and a combination of $CHCl_3$/Et_2O (1/1, v/v), and MeOH/$CHCl_3$ (3/1, v/v), $CHCl_3$/H_2O (1/1, v/v) also failed to give crystals of sufficient quality for single crystal X-ray analysis.

■ ASSOCIATED CONTENT

Supporting Information

The Supporting Information is available free of charge at https://pubs.acs.org/doi/10.1021/acs.jmedchem.0c02194.

Compound molecular formula strings (CSV)

Carboxypeptidase Y assay for NUC-3373_isoB, **10a**, and **10b** (Figures S1a−c); list of primers used for RT-PCR (Table S1); compound purity analyses; and crystal data and structure refinement for the compounds **10a** and **10b** (Table S2) (PDF)

Accession Codes

CCDC 2049153 and 2049154 contain the supplementary crystallographic data for this paper. These data can be obtained free of charge from The Cambridge Crystallographic Data Centre via www.ccdc.cam.ac.uk/structures.

■ AUTHOR INFORMATION

Corresponding Authors

Magdalena Slusarczyk − *Cardiff School of Pharmacy and Pharmaceutical Sciences, Cardiff University, Cardiff CF10 3NB, U.K.;* orcid.org/0000-0002-4707-7190;

https://doi.org/10.1021/acs.jmedchem.0c02194
J. Med. Chem. 2021, 64, 8179−8193

Phone: +44 (0)2920874551; Email: SlusarczykM1@cf.ac.uk

Chris Pepper − *Brighton and Sussex Medical School, University of Sussex, Brighton BN1 9PX, U.K.*; Phone: +44 (0)1273 678644; Email: C.Pepper@bsms.ac.uk

Authors

Michaela Serpi − *Cardiff University, School of Chemistry, Cardiff CF10 3AT, U.K.*

Essam Ghazaly − *Centre for Haemato-Oncology, Barts Cancer Institute, Queen Mary University of London, London EC1M 6BQ, U.K.*

Benson M. Kariuki − *Cardiff University, School of Chemistry, Cardiff CF10 3AT, U.K.*; orcid.org/0000-0002-8658-3897

Christopher McGuigan − *Cardiff School of Pharmacy and Pharmaceutical Sciences, Cardiff University, Cardiff CF10 3NB, U.K.*

Complete contact information is available at: https://pubs.acs.org/10.1021/acs.jmedchem.0c02194

Notes

The authors declare no competing financial interest.

■ ACKNOWLEDGMENTS

The authors would like to thank NuCana plc for funding part of the research work described in this manuscript and Andrew William Gibbs for technical assistance.

■ ABBREVIATIONS USED

BTC, biliary tract cancer; CDA, cytidine deaminase; CSA, camphorsulfonic acid; dCK, deoxycytidine kinase; DPD, dihydropyrimidine dehydrogenase; hENT1, human equilibrative nucleoside transporter 1; TP, thymidine phosphorylase; TS, thymidylate synthase

■ REFERENCES

(1) Cahard, D.; McGuigan, C.; Balzarini, J. Aryloxy phosphoramidate triesters as pro-tides. *Mini-Rev. Med. Chem.* **2004**, *4*, 371−381.

(2) McGuigan, C.; Serpi, M.; Bibbo, R.; Roberts, H.; Hughes, C.; Caterson, B.; Gibert, A. T.; Verson, C. R. A. Phosphate prodrugs derived from N-acetylglucosamine have enhanced chondroprotective activity in explant cultures and represent a new lead in antiosteoarthritis drug discovery. *J. Med. Chem.* **2008**, *51*, 5807−5812.

(3) Serpi, M.; Bibbo, R.; Rat, S.; Roberts, H.; Hughes, C.; Caterson, B.; Alcaraz, M. J.; Gibert, A. T.; Verson, C. R.; McGuigan, C. Novel phosphoramidate prodrugs of N-acetyl-(D)- glucosamine with antidegenerative activity on bovine and human cartilage explants. *J. Med. Chem.* **2012**, *55*, 4629−4639.

(4) Hamon, N.; Quintiliani, M.; Balzarini, J.; McGuigan, C. Synthesis and biological evaluation of prodrugs of 2-fluoro-2-deoxyribose-1-phosphate and 2,2-difluoro-2-deoxyribose-1-phosphate. *Bioorg. Med. Chem. Lett.* **2013**, *23*, 2555−2559.

(5) Hamon, N.; Slusarczyk, M.; Serpi, M.; Balzarini, J.; McGuigan, C. Synthesis and biological evaluation of phosphoramidate prodrugs of two analogues of 2-deoxy-D-ribose-1-phosphate directed to the discovery of two carbasugars as new potential anti-HIV leads. *Bioorg. Med. Chem.* **2015**, *23*, 829−838.

(6) James, E.; Pertusati, F.; Brancale, A.; McGuigan, C. Kinase-independent phosphoramidate S1P1 receptor agonist benzyl ether derivatives. *Bioorg. Med. Chem. Lett.* **2017**, *27*, 1371−1378.

(7) Osgerby, L.; Lai, Y.-C.; Thornton, P. J.; Amalfitano, J.; Le Duff, C. S.; Jabeen, I.; Kadri, H.; Miccoli, A.; Tucker, J. H. R.; Muqit, M. M. K.; Mehellou, Y. Kinetin riboside and its protides activate the Parkinson's disease associated PTEN-induced putative kinase 1 (PINK1) independent of mitochondrial depolarization. *J. Med. Chem.* **2017**, *60*, 3518−3524.

(8) Davey, M. S.; Malde, R.; Mykura, R. C.; Baker, A. T.; Taher, T. E.; Le Duff, C. S.; Willcox, B. E.; Mehellou, Y. Synthesis and biological evaluation of (E)-4-hydroxy-3-methylbut-2-enyl phosphate (HMBP) aryloxy triester phosphoramidate prodrugs as activators of Vγ9/Vδ2 T-cell immune responses. *J. Med. Chem.* **2018**, *61* (5), 2111−2117.

(9) Slusarczyk, M.; Lopez, M. H.; Balzarini, J.; Mason, M.; Jiang, W. G.; Blagden, S.; Thompson, E.; Ghazaly, E.; McGuigan, C. Application of protide technology to gemcitabine: a successful approach to overcome the key cancer resistance mechanisms leads to a new agent (NUC-1031) in clinical development. *J. Med. Chem.* **2014**, *57*, 1531−1542.

(10) McGuigan, C.; Murziani, P.; Slusarczyk, M.; Gonczy, B.; Vande Voorde, J.; Liekens, S.; Balzarini, J. Phosphoramidate protides of the anticancer agent FUDR successfully deliver the preformed bioactive monophosphate in cells and confer advantage over the parent nucleoside. *J. Med. Chem.* **2011**, *54*, 7247−7258.

(11) (a) Mackey, J. R.; Mani, R. S.; Selner, M.; Mowles, D.; Young, J. D.; Belt, J. A.; Crawford, C. R.; Cass, C. E. Functional nucleoside transporters are required for gemcitabine influx and manifestation of toxicity in cancer cell lines. *Cancer Res.* **1998**, *58*, 4349−4357. (b) Gourdeau, H.; Clarke, M. L.; Ouellet, F.; Mowles, D.; Selner, M.; Richard, A.; Lee, N.; Mackey, J. R.; Young, J. D.; Jolivet, J.; Lafrenière, R. G.; Cass, C. E. Mechanisms of uptake and resistance to troxacitabine, a novel deoxycytidine nucleoside analogue, in human leukemic and solid tumor cell lines. *Cancer Res.* **2001**, *61*, 7217−7224.

(12) (a) Ruiz van Haperen, V. W.; Veerman, G.; Eriksson, S.; Boven, E.; Stegmann, A. P.; Hermsen, M.; Vermorken, J. B.; Pinedo, H. M.; Peters, G. J. Development and molecular characterization of a 2′,2′-difluorodeoxycytidine-resistant variant of the human ovarian carcinoma cell line A2780. *Cancer Res.* **1994**, *54*, 4138−4143. (b) Kroep, J. R.; Loves, W. J.; van der Wilt, C. L.; Alvarez, E.; Talianidis, I.; Boven, E.; Braakhuis, B. J. M.; van Groeningen, C. J.; Pinedo, H. M.; Peters, G. J. Pretreatment deoxycytidine kinase levels predict *in vivo* gemcitabine sensitivity. *Mol. Cancer Ther.* **2002**, *1*, 371−376. (c) Galmarini, C. M.; Clarke, M. L.; Jordheim, L.; Santos, C. L.; Cros, E.; Mackey, J. R.; Dumontet, C. Resistance to gemcitabine in a human follicular lymphoma cell line is due to partial deletion of the deoxycytidine kinase gene. *BMC Pharmacol.* **2004**, *4*, 8.

(13) (a) Beumer, J. H.; Eiseman, J. L.; Parise, R. A.; Joseph, E.; Covey, J. M.; Egorin, M. J. Modulation of gemcitabine (2′,2′-difluoro-2′-deoxycytidine) pharmacokinetics, metabolism, and bioavailability in mice by 3,4,5,6-tetrahydrouridine. *Clin. Cancer Res.* **2008**, *14*, 3529−3535. (b) Mini, E.; Nobili, S.; Caciagli, B.; Landini, I.; Mazzei, T. Cellular pharmacology of gemcitabine. *Ann. Oncol.* **2006**, *17*, v7−v12.

(14) Blagden, S. P.; Rizzuto, I.; Suppiah, P.; O'Shea, D.; Patel, M.; Spiers, L.; Sukumaran, A.; Bharwani, N.; Rockall, A.; Gabra, H.; El-Bahrawy, M.; Wasan, H.; Leonard, R.; Habib, N.; Ghazaly, E. Anti-tumour activity of a first-in-class agent NUC-1031 in patients with advanced cancer: results of a phase I study. *Br. J. Cancer* **2018**, *119*, 815−822.

(15) http://www.nucana.com/downloads/NuCana12June2019.pdf (accessed 2019-07-22).

(16) Grem, J. L. 5-Fluorouracil: forty-plus and still ticking. A review of its preclinical and clinical development. *Invest. New Drugs* **2000**, *18*, 299−313.

(17) (a) Zhang, N.; Yin, Y.; Xu, S.-J.; Chen, W.-S. 5-Fluorouracil: mechanisms of resistance and reversal strategies. *Molecules* **2008**, *13*, 1551−1569. (b) Jetté, L.; Bissoon-Haqqani, S.; Le Francois, B.; Maroun, J. A.; Birnboim, C. Resistance of colorectal cancer cells to 5-FUdR and 5-FU caused by mycoplasma infection. *Anticancer Res.* **2008**, *28*, 2175−2180.

(18) Diasio, R. B.; Harris, B. E. Clinical pharmacology of 5-fluorouracil. *Clin. Pharmacokinet.* **1989**, *16*, 215−237.

(19) Vande Voorde, J.; Liekens, S.; McGuigan, C.; Murziani, P. G. S.; Slusarczyk, M.; Balzarini, J. The cytostatic activity of NUC-3073, a phosphoramidate prodrug of 5-fluoro-2'-deoxyuridine, is independent of activation by thymidine kinase and insensitive to degradation by phosphorolytic enzymes. *Biochem. Pharmacol.* **2011**, *82*, 441−452.
(20) Ghazaly, E.; Woodcock, V. K.; Spilipoulou, P.; Spiers, L.; Moschandreas, J.; Griffiths, L.; Gnanaranjan, C.; Harrison, D. J.; Evans, T. R. J.; Blagden, S. *42nd ESMO Congress 2017*, Madrid, Spain, September 8−12, 2017; 385-P.
(21) https://clinicaltrials.gov/ct2/show/NCT03428958 (accessed 2019-03-28).
(22) https://clinicaltrials.gov/ct2/show/NCT03829254 (accessed 2019-08-28).
(23) (a) Pradere, U.; Garnier-Amblard, E. C.; Coats, S. J.; Amblard, F.; Schinazi, R. F. Synthesis of nucleoside phosphate and phosphonate prodrugs. *Chem. Rev.* **2014**, *114*, 9154−9218. (b) Slusarczyk, M.; Serpi, M.; Pertusati, F. Phosphoramidates and phosphonamidates (protides) with antiviral activity. *Antivir. Chem. Chemother.* **2018**, DOI: 10.1177/2040206618775243.
(24) Simmons, B.; Liu, Z.; Klapars, A.; Bellomo, A.; Silverman, S. M. Mechanism-based solution to the protide synthesis problem: selective access to sofosbuvir, acelarin, and INX-08189. *Org. Lett.* **2017**, *19*, 2218−2221.
(25) Singh, H.; Bhatia, H.; Grewal, N.; Natt, N. Sofosbuvir: A novel treatment option for chronic hepatitis C infection. *J. Pharmacol. Pharmacother.* **2014**, *5*, 278−282.
(26) Sofia, M. J.; Bao, D.; Chang, W.; Du, J.; Nagarathnam, D.; Rachakonda, S.; Reddy, P. G.; Ross, B. S.; Wang, P.; Zhang, H. R.; Bansal, S.; Espiritu, C.; Keilman, M.; Lam, A. M.; Steuer, H. M.; Niu, C.; Otto, M. J.; Furman, P. A. Discovery of a β-d-2-Deoxy-2-α-fluoro-2-β-C-methyluridine nucleotide prodrug (PSI-7977) for the treatment of hepatitis C virus. *J. Med. Chem.* **2010**, *53*, 7202−7218.
(27) Ray, A. S.; Fordyce, M. W.; Hitchcock, M. J. M. Tenofovir alafenamide: a novel prodrug of tenofovir for the treatment of human immunodeficiency virus. *Antiviral Res.* **2016**, *125*, 63−70.
(28) Lee, W. A.; He, G. X.; Eisenberg, E.; Cihlar, T.; Swaminathan, S.; Mulato, A.; Cundy, K. C. Selective intracellular activation of a novel prodrug of the human immunodeficiency virus reverse transcriptase inhibitor tenofovir leads to preferential distribution and accumulation in lymphatic tissue. *Antimicrob. Agents Chemother.* **2005**, *49*, 1898−1906.
(29) Nguyen, L. A.; He, H.; Pham-Huy, C. Chiral drugs: an overview. *Int. J. Biomed. Sci.* **2006**, *2*, 85−100.
(30) https://www.fda.gov/regulatory-information/search-fda-guidance-documents/development-new-stereoisomeric-drugs (accessed 20121-02-23).
(31) Roman, C. A.; Balzarini, J.; Meier, C. Diastereoselective synthesis of aryloxy phosphoramidate prodrugs of 3′-deoxy-2′,3′-didehydrothymidine monophosphate. *J. Med. Chem.* **2010**, *53*, 7675−7681.
(32) Ross, B. S.; Ganapati Reddy, P.; Zhang, H.-R.; Rachakonda, S.; Sofia, M. J. Synthesis of diastereomerically pure nucleotide phosphoramidates. *J. Org. Chem.* **2011**, *76*, 8311−8319.
(33) *Synthesis of substantially diastereomerically pure phosphate protides*. WO Patent 2018/229493, 2018.
(34) *Diastereoselective synthesis of phosphate derivatives and of the gemcitabine prodrug NUC-1031*. WO Patent 2017/098252 A1, 2017.
(35) Pertusati, F.; McGuigan, C. Diastereoselective synthesis of P-chirogenic phosphoramidate prodrugs of nucleoside analogues (protides) via copper catalysed reaction. *Chem. Commun.* **2015**, *51*, 8070−8073.
(36) Zhu, X.-F.; Williams, H. J.; Scott, A. I. Facile and highly selective 5′-desilylation of multisilylated nucleosides. *Chem. Soc. Perkin. Trans 1* **2000**, 2305−2306.
(37) Chandrasekhar, S.; Srihari, P.; Nagesh, C.; Kiranmai, N.; Nagesh, N.; Idris, M. M. Synthesis of readily accessible triazole-linked dimer deoxynucleoside phosphoramidite for solid-phase oligonucleotide synthesis. *Synthesis* **2010**, *2010* (21), 3710−3714.
(38) Chandrasekhar, S.; Rambabu, C.; Reddy, A. S. Spirastrellolide B: the synthesis of southern (C_9−C_{25}) region. *Org. Lett.* **2008**, *10*, 4355−4357.
(39) (a) Wang, D.; Zou, L.; Jin, Q.; Hou, J.; Ge, G.; Yang, L. Human carboxylesterases: a comprehensive review. *Acta Pharm. Sin. B* **2018**, *8*, 699−712. (b) Imai, T.; Taketani, M.; Shii, M.; Hosokawa, M.; Chiba, K. Substrate specificity of carboxylesterase isozymes and their contribution to hydrolase activity in human liver and small intestine. *Drug Metab. Dispos.* **2006**, *34*, 1734−1741.
(40) Birkus, G.; Wang, R.; Liu, X.; Kutty, N.; MacArthur, H.; Cihlar, T.; Gibbs, C.; Swaminathan, S.; Lee, W.; McDermott, M. Cathepsin A is the major hydrolase catalyzing the intracellular hydrolysis of the antiretroviral nucleotide phosphonoamidate prodrugs GS-7340 and GS-9131. *Antimicrob. Agents Chemother.* **2007**, *51*, 543−550.
(41) Lapidot, T.; Sirard, C.; Vormoor, J.; Murdoch, B.; Hoang, T.; Caceres-Cortes, J.; Minden, M.; Paterson, B.; Caligiuri, M. A.; Dick, J. E. A cell initiating human acute myeloid leukaemia after transplantation into SCID mice. *Nature* **1994**, *367*, 645−648.
(42) Phi, L. T. H.; Sari, I. N.; Yang, Y.-G.; Lee, S.-H.; Jun, N.; Kim, K. S.; Lee, Y. K.; Kwon, H. Y. Cancer stem cells (CSCs) in drug resistance and their therapeutic implications in cancer treatment. *Stem Cells Int.* **2018**, *2018*, 5416923.
(43) Paschall, A. V.; Yang, D.; Lu, C.; Redd, P. S.; Choi, J.-H.; Heaton, C. M.; Lee, J. R.; Nayak-Kapoor, A.; Liu, K. $CD133^+CD24^{lo}$ defines a 5-fluorouracil-resistant colon cancer stem cell-like phenotype. *Oncotarget* **2016**, *7*, 78698−78712.
(44) Van den broeck, A.; Gremeaux, L.; Topal, B.; Vankelecom, H. Human pancreatic adenocarcinoma contains a side population resistant to gemcitabine. *BMC Cancer* **2012**, *12*, 354.
(45) Zeijlemaker, W.; Grob, T.; Meijer, R.; Hanekamp, D.; Kelder, A.; Carbaat-Ham, J. C.; Oussoren-Brockhoff, Y. J. M.; Snel, A. N.; Veldhuizen, D.; Scholten, W. J.; Maertens, J.; Breems, D. A.; Pabst, T.; Manz, M. G.; van der Velden, V. H. J.; Slomp, J.; Preijers, F.; Cloos, J.; van de Loosdrecht, A. A.; Löwenberg, B.; Valk, P. J. M.; Jongen-Lavrencic, M.; Ossenkoppele, G. J.; Schuurhuis, G. J. $CD34^+$ $CD38^-$ leukemic stem cell frequency to predict outcome in acute myeloid leukemia. *Leukemia* **2019**, *33*, 1102−1112.
(46) Hagmann, W.; Jesnowski, R.; Löhr, J. M. Interdependence of gemcitabine treatment, transporter expression, and resistance in human pancreatic carcinoma cells. *Neoplasia* **2010**, *12*, 740−747.
(47) Yao, L.; Gu, J.; Mao, Y.; Zhang, X.; Wang, X.; Jin, C.; Fu, D.; Li, J. Dynamic quantitative detection of ABC transporter family promoter methylation by MS-HRM for predicting MDR in pancreatic cancer. *Oncol. Lett.* **2018**, *15*, 5602−5610.
(48) Corcoran, D. B.; Lewis, T.; Nahar, K. S.; Jamshidi, S.; Fegan, C.; Pepper, C.; Thurston, D. E.; Rahman, K. M. Effects of systematic shortening of noncovalent C8 side chain on the cytotoxicity and NF-κB inhibitory capacity of pyrrolobenzodiazepines (PBDs). *J. Med. Chem.* **2019**, *62*, 2127−2139.
(49) Sheldrick, G. M. A short history of *SHELX*. *Acta Crystallogr., Sect. A: Found. Crystallogr.* **2008**, *64*, 112−122.
(50) Sheldrick, G. M. *SHELXT* − Integrated space-group and crystal-structure determination. *Acta Crystallogr., Sect. C: Struct. Chem.* **2015**, *71*, 3−8.